CATALYTIC STEAM CRACKING OF N-HEXANE OVER PT CATALYSTS

TEERUD PANJANAPONGCHAI

A THESIS SUBMITTED IN PARTIAL FULFILLMENT OF THE REQUIREMENT FOR THE DEGREE OF MASTER OF SCIENCE IN APPLIED CHEMISTRY

DEPARTMENT OF CHEMISTRY SCHOOL OF SCIENCE

KING MONGKUT'S INSITUTE OF TECHNOLOGY LADKRABANG 2022

KMITL-2022-SC-M-012-096

Thesis Title	Catalytic steam cracking of n-Hexane over Pt catalysts
Student Name	Mr. Teerud Panjanapongchai
Student ID	60605028
Degree	Master of science (Applied Chemistry)
Department	Chemistry
Year	2022
Thesis Advisor	Professor Dr. Tawan Sooknoi
Thesis Co-advisor	Associate Professor Dr. Tosapol Maluangnont

Abstract

The conversion of naphtha into chemical feedstocks such as ethylene or propylene is of interest for petrochemical industries. Naphtha typically consists of hydrocarbons of six carbons or less (light naphtha) or more than that (heavy naphtha). Here, several platinum-based supported catalysts were evaluated in catalytic cracking of n-hexane as a model for naphtha feed in the presence of stream. Variables to be investigated include the reaction temperature configuration in the three-zone furnace and space-velocity of the n-hexane. The catalysts studied included 0.5Pt/TiO_2, 0.5Pt/ZrO_2 and 0.5Pt/SiO_2 were prepared and characterized by XRD, N_2-physisorption, ICP, TEM and H_2-TPR. Among all tested catalysts, 0.5Pt/SiO_2 with the largest particle size exhibits the highest n-hexane cracking activity. In addition, it was observed by TEM of 0.5Pt/TiO_2 that longer reduction time results in larger Pt particles sizes which enhanced the cracking activity.

Keywords: n-Hexane, steam cracking, supported Pt catalyst, ethylene

Acknowledgement

The author desires to appreciatively thank my advisors, Professor Dr. Tawan Sooknoi and Associate Professor Dr. Tosapol Maluangnont for suggestions, inspiration, carefulness, reassurance, experimental instrument, and knowledge in catalysis throughout this research.

I would like to gratefully acknowledge chairperson and committee, Associate Professor Dr. Siriporn Jongpatiwut and Associate Professor Dr. Punnama Siriphannon for judgment and valuable comments.

Moreover, I would like to acknowledge the financial support from SCG Chemicals Co. Ltd. In addition, I would like to thank School of Science and Catalytic Chemistry Research Unit, King Mongkut's Institute of Technology Ladkrabang for the equipment, chemicals, and facilities.

Unforgettable, I would like to grateful to my colleague in Catalytic Chemistry Research Unit (CCR group) for their help, advice, support, and encouragement.

Finally, I deeply appreciate and thank my family for their love and support.

Mr. Teerud Panjanapongchai

Table of contents

List of tables

List of figures

List of schemes

Chapter 1

Introduction

1.1 Motivation

Light olefins, such as ethylene and propylene, are very important building blocks of the petrochemical industry. Their worldwide demands and consumption are increasing [1,2]. They are mostly produced by steam cracking of naphtha. Typically, naphtha is carried with steam as a diluent for naphtha cracking which can reduce the coke deposition effectively. The thermal cracking of naphtha consumes more than 30% of the total amount of energy required in petrochemical refinement. Accordingly, developing efficient processes for the production of light olefins is indispensable. The catalytic cracking process is the alternative way to reduce energy cost and provide selective production of olefins.

For either thermal or catalytic cracking, catalyst deactivation is mainly caused by coke deposition [3-6]. The cracking catalyst for high yield of olefins typically consists of Y-zeolite, active alumina, and an inert binder. The catalysts are facing two problems to be overcome: dealumination of Y-zeolite and coke deposition [7]. The alternative choices for cracking catalysts are precious metals and composite oxide catalysts. Such noble metal catalysts have some shortcomings, such as susceptibility to poisoning, high prices, deactivation by carbon deposition [8]. In this research, supported Pt catalysts including 0.5%Pt/SiO_2, 0.5%Pt/TiO_2 and 0.5%Pt/ZrO_2 will be tested for catalytic steam cracking of *n*-hexane to light olefins. The effects of temperature, temperature configuration of the 3-zone furnace, and linear hour space velocity (LHSV) on activity and stability were investigated.

1.2 Objectives

1) To enhance olefins yield from *n*-hexane via catalytic steam cracking reaction
2) To understand the effect of temperature configuration of the 3-zone furnace and linear hour space velocity (LHSV) on *n*-hexane steam cracking
3) To understand the effect of support on the conversion of *n*-hexane to olefins over Pt catalysts
4) To understand the reducing time effect of 0.5Pt/TiO_2 on the Pt particle size and activity

1.3 Scopes of study

1) Preparation of supported Pt catalysts by incipient wetness impregnation techniques using various support including TiO_2, ZrO_2 and SiO_2.
2) Characterization of the catalysts by X-ray diffraction (XRD), inductively coupled plasma atomic emission spectroscopy (ICP-AES), nitrogen adsorption/desorption, temperature programmed reduction (TPR) and transmission electron microscopy (TEM)
3) Study the conversion of *n*-hexane in a continuous fixed-bed reactor by varying temperature configuration of the 3-zone furnace, feed rate (LHSV), Pt Supporter (TiO_2, ZrO_2 and SiO_2) and catalyst reducing time.
4) Study on catalyst stability (6 hours on steam)
5). Products were analyzed and identified by off-line and on-line Gas Chromatography with flame ionization detector (GC-FID).

1.4 Expected result

The finding from this project can offer alternative choice of metal-containing catalyst that enhances olefins yield while also increases catalyst stability for catalytic steam cracking of naphtha by using *n*-hexane as feed model.

Chapter 2

Theory and Literature Reviews

2.1 Naphtha

Petroleum naphtha is an intermediate hydrocarbon liquid stream derived from the refining of crude oil [9,10,11] with CAS-no 64742-48-9 [12]. It is most usually desulfurized and then catalytically reformed, which rearranges or restructures the hydrocarbon molecules in the naphtha as well as breaking some of the molecules into smaller molecules to produce a high-octane component of gasoline (or petrol). Naphtha is a mixture of many different hydrocarbon compounds. It has an initial boiling point (IBP) of about 35 °C and a final boiling point (FBP) of about 200 °C, and it contains paraffins, naphthenes (cyclic paraffins) and aromatic hydrocarbons ranging from those containing 4 carbon atoms to those containing about 10 or 11 carbon atoms.

The virgin naphtha is often further distilled into two streams:

1. a virgin light naphtha with an IBP of about 30 °C and a FBP of about 145 °C containing most (but not all) of the hydrocarbons with six or fewer carbon atoms
2. a virgin heavy naphtha containing most (but not all) of the hydrocarbons with more than six carbon atoms. The heavy naphtha has an IBP of about 140 °C and a FBP of about 205 °C.

Some petroleum refineries also produce small amounts of specialty naphthas for use as solvents, cleaning fluids and dry-cleaning agents, paint and varnish diluents, asphalt diluents, rubber industry solvents, recycling products, and cigarette-lighter, portable-camping-stove and lantern fuels. Those specialty naphthas are subjected to various purification processes which adjust chemical characteristics to suit specific needs. Petroleum naphtha is also used in the petrochemicals industry as feedstock to steam reformers and steam crackers for the production of hydrogen (which is converted into

ammonia for fertilizers), ethylene, and other olefins. Natural gas is also used as feedstock to steam reformers and steam crackers [13].

2.2 *n*-Hexane

n-Hexane is a significant constituent of gasoline. It is a colorless liquid, odorless when pure, and with boiling points approximately 69 °C. *n*-Hexane is a chemical made from crude oil. *n*-Hexane is an organic compound, a straight-chain alkane with six carbon atoms and has the molecular formula C_6H_{14}. It is a colorless liquid with a slightly disagreeable odor, highly flammable, and its vapors can be explosive. Pure *n*-hexane is used in laboratories. Most of the hexane used in industry is mixed with similar chemicals called solvents. The major use for solvents containing *n*-hexane is to extract vegetable oils from crops such as soybeans. These solvents are also used as cleaning agents in the printing, textile, furniture, and shoemaking industries. Certain kinds of special glues used in the roofing and shoe and leather industries also contain *n*-hexane. Several consumer products contain *n*-hexane, such as gasoline, quick-drying glues used in various hobbies, and rubber cement [14]. Because light naphtha containing most hydrocarbon with six of fewer carbon atoms, *n*-hexane was used as light naphtha feed model for steam cracking in this project.

2.3 Olefins

2.3.1 Ethylene

Ethylene ($H_2C=CH_2$) is the simplest of the organic compounds known as alkenes, which contain carbon-carbon double bonds. It is a colorless, flammable gas having a sweet taste and odor. Ethylene is an important industrial organic chemical. Ethylene is produced by several methods in the petrochemical industry. A primary method is steam cracking (SC) where hydrocarbons and steam are heated to 750–950 °C. This process converts large hydrocarbons into smaller ones and introduces unsaturation. When ethane is the feedstock, ethylene is the product. Ethylene is separated from the resulting mixture by repeated compression and distillation [15]. In Europe and Asia, ethylene is obtained mainly

from cracking naphtha, gasoil and condensates with the coproduction of propylene, C4 olefins and aromatics (pyrolysis gasoline) [16]. Other technologies employed for the production of ethylene include oxidative coupling of methane, Fischer-Tropsch synthesis, methanol-to-olefins (MTO), and catalytic dehydrogenation [17].

Ethylene is widely used in the chemical industry, and its worldwide production (over 150 million tons in 2016 [18]) exceeds that of any other organic compound [19,20]. Much of this production goes toward polyethylene, a widely used plastic containing polymer chains of ethylene units in various chain lengths. The other industrial reactions of ethylene are 1) oxidation, 2) halogenation and hydrohalogenation, 3) alkylation, 4) hydration, 5) oligomerization, and 6) hydroformylation [21].

2.3.2 Propylene

Propylene is an unsaturated organic compound with the chemical formula $CH_3CH=CH_2$. It has one double bond. It is a colorless gas with a faint petroleum-like odor [22]. The dominant technology for producing propylene is steam cracking. The feedstock is naphtha or propane, especially in the Middle East, where there is an abundance of propane from oil/gas operations [23]. Propylene can be separated by fractional distillation from hydrocarbon mixtures obtained from cracking and other refining processes; refinery-grade propene is about 50 to 70% [24]. In the United States, shale gas is a major source of propane.

Propene is the second most important starting product in the petrochemical industry after ethylene. It is the raw material for a wide variety of products. Polypropylene manufacturers consume nearly two thirds of global production [25]. Polypropylene end uses include films, fibers, containers, packaging, and caps and closures. Propene is also used for the production of important chemicals such as propylene oxide, acrylonitrile, cumene, butyraldehyde, and acrylic acid. In the year 2013 about 85 million tons of propene were processed worldwide [26].

2.4 Steam cracking

Steam cracking is a petrochemical process in which saturated hydrocarbons are broken down into smaller, often unsaturated, hydrocarbons. It is the principal industrial method for producing the lighter alkenes (or commonly olefins), including ethylene and propylene. Steam cracker units are facilities in which a feedstock such as naphtha, liquefied petroleum gas (LPG), ethane, propane or butane is thermally cracked through the use of steam to produce lighter hydrocarbons.

In steam cracking, a gaseous or liquid hydrocarbon feed like naphtha, LPG, or ethane is diluted with steam and briefly heated in a furnace in the absence of oxygen [27]. Typically, the reaction temperature is very high, at around 850 °C. The reaction occurs rapidly: the residence time is on the order of milliseconds. After the cracking temperature has been reached, the gas is quickly quenched to stop the reaction in a transfer line heat exchanger or inside a quenching header using quench oil [28]. The products produced in the reaction depend on the composition of the feed, the hydrocarbon-to-steam ratio, and on the cracking temperature and furnace residence time. Light hydrocarbon feeds such as ethane, LPGs, or light naphtha give mainly lighter alkenes, including ethylene, propylene, and butadiene. Heavier hydrocarbon (full range and heavy naphthas as well as other refinery products) feeds give some of these same products, but also those rich in aromatic hydrocarbons and hydrocarbons suitable for inclusion in gasoline or fuel oil. A higher cracking temperature (also referred to as severity) favors the production of ethene and benzene, whereas lower severity produces higher amounts of propene, C4-hydrocarbons and liquid products. The process also results in the slow deposition of coke, a form of carbon, on the reactor walls. This degrades the efficiency of the reactor, such that reaction conditions are designed to minimize this. Nonetheless, a steam cracking furnace can usually only run for a few months at a time between de-coking. Decoke requires the furnace to be isolated from the process and then a flow of steam or a steam/air mixture is passed through the furnace coils. This converts the hard solid carbon layer to carbon monoxide and carbon dioxide. Once this reaction is complete, the furnace can be returned to service [29].

2.5 *n*-Hexane cracking mechanism

For typical *n*-hexane cracking, the reaction proceeds via radical mechanism, initiated by homolytic cleavage of C-C bond or C-H bond. First possibility is the C2-C3 cleavage of *n*-hexane which produces ethyl radical and butyl radical as shown in **scheme 1**.

Scheme 1 C2-C3 cleavage of *n*-hexane

The primary butyl radical can undergo β-scissions to produce ethylene (**scheme 2**) and another ethyl radical. However, most of ethylene is produced via the C-H cleavage of the ethyl radical (**scheme 3**).

Scheme 2 β-scissions of the butyl radical

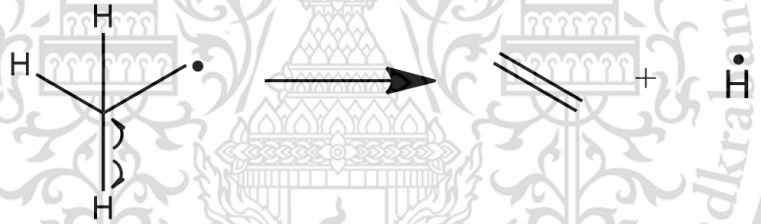

Scheme 3 C-H cleavage of the ethyl radical

The second possibility is C3-C4 cleavage of *n*-hexane which to produce 2 equivalents of primary propyl radical as shown in **scheme 4**.

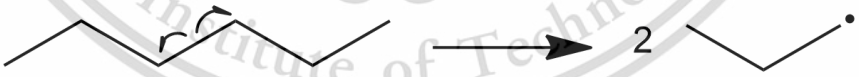

Scheme 4 C3-C4 cleavage of n-Hexane

In this case, the formed propyl radical can undergo β-scissions to produce ethylene and methyl radical (**scheme 5**) that can abstract hydrogen from another hydrocarbon to form methane (**scheme 6**).

Scheme 5 β-scissions of the propyl radical

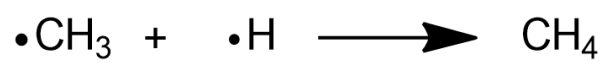

Scheme 6 H-abstraction of the methyl radical

Although, most of propylene is produced via the C-H cleavage of the propyl radical as shown in **scheme 7**.

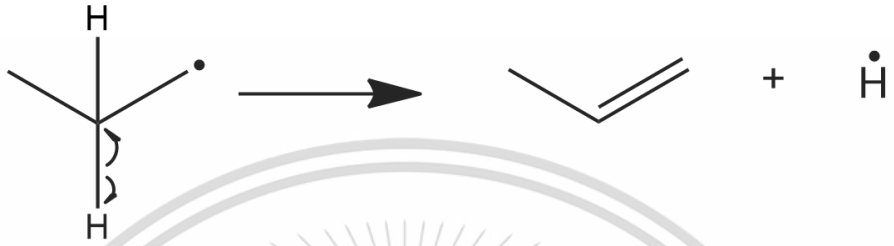

Scheme 7 C-H cleavage of the propyl radical

The third possibility is C1-C2 cleavage of *n*-hexane which produces methyl radical and pentyl radical as shown in **scheme 8**.

Scheme 8 C1-C2 cleavage of *n*-hexane

The pentyl radical can undergo β-scissions to produce ethylene and primary propyl radical which can produce propylene as shown in **scheme 9** or C-H cleavage to form pentene (**scheme 10**).

Scheme 9 β-scissions of the pentyl radical

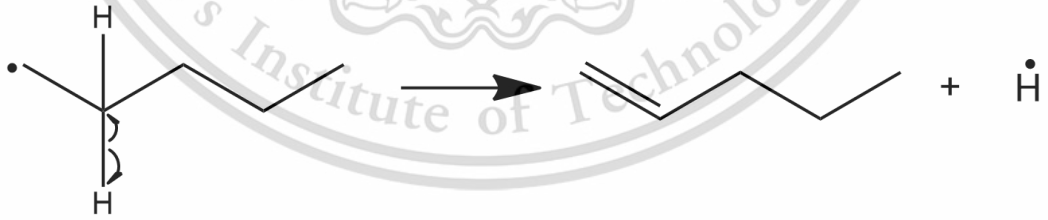

Scheme 10 C-H cleavage of the pentyl radical

Both 1-butene and 1-pentene also convert to butadiene. Hydrogen abstraction from 1-butene leads to the formation of the allylic 1-buten-3-yl radical, while the C-H cleavage of this specie yields butadiene as shown in **scheme 11**.

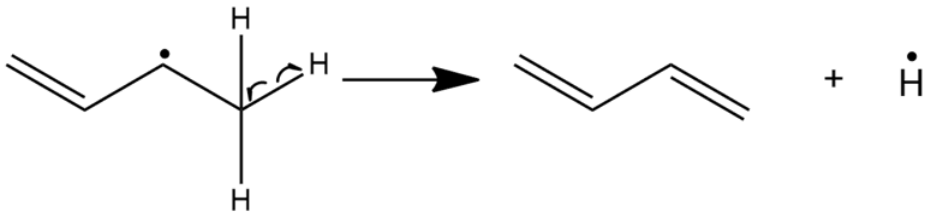

Scheme 11 C-H cleavage of the 1-buten-3-yl radical

Hydrogen abstraction from 1-pentene leads to the formation of the allylic 1-penten-3-yl radical. The subsequent β-scissions of this radical also forms butadiene as shown in **scheme 12**.

Scheme 12 β-scissions of the secondary 1-penten-3-yl radical

In addition, these radical intermediates can couple with another alkyl radical to form larger molecule or undergo hydrogen abstraction which lead to their stabilization.

2.6 Literature review

Steam cracking is a petrochemical process in which saturated hydrocarbons are broken down into smaller, often unsaturated, hydrocarbons. It is the principal industrial method for producing lighter alkenes (olefins), including ethylene and or propylene. Steam cracker units are facilities in which a feedstock such as naphtha, liquefied petroleum gas (LPG), ethane, propane or butane is thermally cracked through the use of steam to produce lighter hydrocarbons.

In 1998 S.M. Babitz [30] studied the cracking activity of *n*-hexane over zeolite catalysts including HZSM-5, H-MOR and H-USY. The reaction was investigated at 480-540°C. The result confirmed that catalytic cracking with zeolite catalyst was affected by the differences in the concentration of adsorbed alkane in zeolite pores which enhance the cracking activity. However, zeolite catalyst is not suitable for steam cracking because it is not tolerant to high temperature and steam atmospheric which resulted in the collapse of the structure.

In 2014 A. Yamaguchi [31] studied the deactivation of ZSM-5 zeolite during catalytic steam cracking of *n*-hexane. The reaction conditions were the following: temperature at

650°C, WHSV (hexane) 11h^{-1}, W/F 8 $g_{catalyst}h/mol_{hexane}$. The HZSM-5 catalysts showed high initial cracking activity but deactivated rapidly during the steam cracking. The deactivation is mainly caused by dealumination. Moreover, the deactivation is also affected by the deposited coke which could be removed by calcination.

In 2016 Sungwon Lee [32] studied the effect of Pt particle size on catalytic cracking of *n*-dodecane over Pt/SiO_2 catalyst. The reaction was investigated at 400-600°C. The reactivity of supported Pt catalysts is dependent on the Pt particle size. The results suggest that controlling the size and geometric structure of Pt particle could influence the catalytic performance.

Chapter 3

Experimental

3.1 Reagents

Table 3.1 Materials and chemicals

Chemicals	Grade of purity	Manufactures
1. Nitrogen gas	99.999%	UIG
2. Air zero gas		UIG
3. Hydrogen gas	99.995%	UIG
4. Deionized water		KHUNCHORN TECHNOLOGY
5. *n*-Hexane	95.00%	CARLO ERBA
6. Dodecane	99.00%	ACROS
7. Benzene	99.70%	SIGMA-ALDRICH
8. Cyclohexane	99.70%	RFCL
9. *n*-Heptane	99.00%	CARLO ERBA
10. Toluene	99.80%	CARLO ERBA
11. *n*-Octane	99.00%	CARLO ERBA
12. Ethylbenzene	99.00%	MERCK
13. Xylene	98.50%	CARLO ERBA
14. Chloroplatinic acid hexahydrate	99.8% Trace metal basis	SIGMA-ALDRICH
15. Zirconium (IV) oxide	98.50%	THERMO SCIENCITIFIC
16. SiO_2, davisil grade		SIGMA-ALDRICH
17. TiO_2, anatase	99.80%	SIGMA-ALDRICH

3.2 Apparatus

1. Mass flow controller (BROOKS INSTRUMENT LLC, Model SLA5350SB1AB1B2A1D3N4AA)
2. 3-Zone Tube furnace with a programmed temperature controller (UTSAKAN, Model VIF)
3. Tube furnace with a programmed temperature controller (VECSTAR, Model VCTF4)
4. Muffle furnace with a programmed temperature controller
5. Gas chromatograph (Varian, Model 3400)
6. Gas chromatograph (AGILENT TECHNOLOGIES, Model 6890)
7. Capillary column (AGILENT TECHNOLOGIES, Model HP-PLOT)
8. Capillary column (RESTEK, Model MXT-1)
9. Sieve (U.S.A standard sieve, Model AASHO N-92)
10. Temperature programmed reduction (TPR, Model TCD2-NIFED)
11. X-ray powder diffractometer (XRD, Rigaku, DMAX 2200/Ultima+)
12. Element Analyzer ICP-OES Model Avio500.
13. Gas Adsorption Analyzer (Autosorb-1C, Quantachrome)
14. Transmission electron microscope (JEOL JEM-2100)
15. Syringe (50mL)
16. Syringe pump
17. Laboratory glassware
18. Laboratory plasticware
19. Oven

3.3 Experimental procedure

3.3.1 Catalyst preparation

3.3.1.1 Supports (TiO_2, SiO_2, ZrO_2)

All supports, including TiO_2 (Sigma-Aldrich, 99.8% trace metal basis), SiO_2 (Sigma-Aldrich, davisil high purity grade) and ZrO_2 (Thermo Scientific™, 98.5%) were calcined in muffle furnace under typical laboratory atmosphere at 600˚C for 4 h.

3.3.1.2 Pt catalysts (0.5Pt/TiO_2, 0.5Pt/SiO_2, 0.5Pt/ZrO_2)

The 0.5 wt.% Pt/TiO_2, 0.5 wt.% Pt/SiO_2 and 0.5 wt.% Pt/ZrO_2 catalysts were prepared by impregnation method using 0.105 g of $H_2PtCl_6{\cdot}xH_2O$ (Sigma-Aldrich, 99.995% trace metal basis) in 12 mL deionized water. This solution was slowly added dropwise to 9.95 g of the calcined support. Then, the catalyst was dried overnight at 80˚C and then calcined in air at 600˚C for 4 h. Subsequently, the catalyst was reduced in H_2 at 600˚C for 5 h.

3.3.2 Catalyst characterization

3.3.2.1 Structural analysis using X-ray diffraction (XRD)

The crystalline phase of the prepared catalysts were identified using X-ray diffractometer (Rigaku, DMAX 2200/Ultima+, Faculty of Science, Chulalongkorn University). The sample was ground before it was packed on the sample holder. Analysis was done covering the range of 2Theta = 10-70˚, at the rate of 0.02˚/step, and the scanning rate of 1 s/step.

3.3.2.2 Determination of specific surface area by nitrogen adsorption/desorption

Specific surface area of the catalysts were determined by a gas adsorption analyzer (Autosorb-1C, Quantachrome). Approximately 0.01-0.05 g of the sample was loaded into the cell, which is attached to the outgassing station equipped with a heating mantle. The

temperature was raised to 350°C during outgassing process. After that, nitrogen gas was introduced to the sample cell where the adsorption can be measured at the range of the partial pressure (P/P_0) from 10^{-6} to 1.0. The adsorption isotherm and the corresponding surface area was analyzed using BET **equation** as shown in **Equation 3.1.**

$$\frac{1}{\upsilon\,[(p_0/p)-1]} = \frac{c-1}{\upsilon_m c}\left(\frac{p}{p_0}\right) + \frac{1}{\upsilon_m c}$$

Equation 3.1

Where P and P_0 are the equilibrium and the saturation pressure of adsorbents at the temperature of adsorption, υ_m is the adsorbed gas quantity (for example, in volume units), υ_m is the monolayer adsorbed gas quantity, and C is the BET constant.

3.3.2.3 Quantitative elemental composition analysis by inductively coupled plasma atomic emission spectroscopy (ICP-AES)

Inductively coupled plasma atomic emission spectroscopy was used to measure the Pt content. The particles were digested in aqua regia solution with periodic agitation for 24 h to ensure complete dissolution. The dissolved metal content, in parts per million, was measured using an Element Analyzer ICP-OES Model Avio500.

3.3.2.4 Morphology, structure, dispersion of metal in the catalysts by transmission electron microscopy (TEM)

Morphology and Pt dispersion of the catalysts were investigated by transmission electron microscope (JEOL JEM-2100). The sample specimens for TEM experiment were prepared by dispersing the catalyst powder in ethanol, followed by dropping on holey carbon film supported by a copper grid. The samples were put into the TEM instrument which uses a beam of highly energetic electron (voltage 200 kV). Electrons that pass through the sample without energy loss shows bright filed image and electrons are diffracted (scattered) by particles to obtain dark-field images at magnification of 100,000 – 120,000x.

3.3.2.5 Temperature programmed reduction (H_2-TPR)

Temperature programmed reduction was measured using a thermal conductivity detector (TCD). The sample weighed 0.2 g was placed into a quartz tube reactor, which was located inside a temperature-regulated furnace. Prior to the H_2-TPR, each sample was heated to its activation temperature 100°C in nitrogen for 2 h at 10°C/min and was cooled down to below 50°C. The heating rate of 10°C/min and 30 mL/min of 10% H_2 in Ar was applied for TPR analysis. Water production during the reduction process was removed in a U-shape glass trap at -95°C (vapor of liquid N_2) before entering the TCD.

3.3.3 Catalytic activity testing

Catalytic conversion of *n*-hexane was carried out at atmospheric pressure in a fixed-bed continuous-flow quartz reactor (8 mm) in a three-zone temperature-controlled furnace. The catalyst powders were pelletized and crushed to the desired size (600-850 μm). After that, it was packed into a quartz tube reactor and covered with quartz wool and quartz rods. Gas flow rate was controlled by a mass flow controller. Before the catalytic reaction, the as-prepared catalysts were pretreated at 600°C for 1 h in air zero (60 ml/h) and reduced at 600°C for 5.5 h in hydrogen flow (60 ml/h). *n*-Hexane and water (weight ratio of 0.9) were separately introduced into the reactor using syringe pumps. The catalytic testing was conducted for a total time on stream (TOS) of 6 h. The scheme of catalytic testing rig is shown in Figure 1.

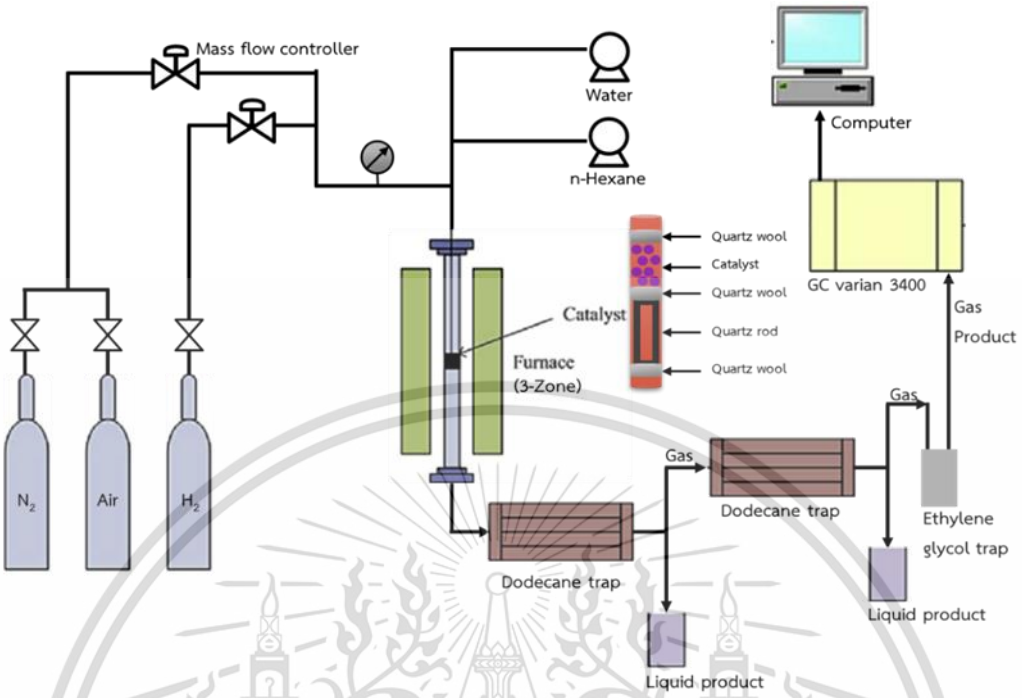

Figure 1 Steam catalytic cracking experimental setup scheme.

3.3.4 Products analysis

The coke deposit on catalysts were determined by weighing the quartz reactor (including catalyst and packings) before and after reaction. The difference in weight was used for calculating the coke product as shown by **Equation 3.2**.

$$\text{Solid product, coke (g)} = \frac{[\text{Tube after run (g)} - \text{Tube before run (g)}] \times 100}{\text{Feed per run (g)}}$$

Equation 3.2

The liquid products were periodically trapped with dodecane every 3 h. The liquid products (collected in 50ml volumetric flask) were spiked with 1.00 mL of cyclohexane which serves as the internal standard, followed by volume adjustment to 50 mL. The liquid product was analyzed by gas chromatograph (GC-FID, Agilent 6890) equipped with MXT-1 capillary column. The temperature of the injection port was set at 250 °C, 40 °C for column oven, and 250 °C for FID detector. The GC temperature condition started at 40 °C, hold for 5 min then heated up to 280 °C with a heating rate 15 °C/min, followed by a final hold for 2 min. Pressure of the carrier gas was fixed to 5 psi at all time. The products were

recorded as a chromatogram, where the peak area could be electronically measured and calculated. By comparing with the retention time of the standard and the internal standard peak areas, the species and composition of each product can be successfully determined by **Equation 3.3**.

$$\text{Liquid product (g)} = \frac{\left(\frac{\text{Product area in sample}}{\text{Cyclohexane area in sample}}\right)}{\left(\frac{\text{Product area in standard}}{\text{Cyclohexane area in standard}}\right)} \text{x Product weight in standard (g)}$$

Equation 3.3

Meanwhile, non-condensed gas product was analyzed by an on-line by a gas chromatograph (GC-FID Varian 3400) equipped with HP-PLOT capillary column. The products were collected in a gas sampling loop, and then periodically injected into the GC column with an inert carrier nitrogen gas. The temperature of the injection port was set at 250°C, 35°C for column oven, and 250°C for FID detector. The GC temperature condition was started at 35 °C, hold for 1.5 min, heating up to 100 °C with heating rate 5 °C/min, heating up to 180 °C/min with heating rate 10, and a final hold for 5.5 min. Pressure of the carrier gas was fixed to 5 psi at all time. The products were recorded as a chromatogram. Each peak area was measured and calculated. Comparing with standard peak areas, the species and composition of each product can be determined in **Equation 3.4 and 3.5**.

$$\text{Gas product (\%)} = 100 - \%\text{Solid Product} - \%\text{Liquid Product}$$

Equation 3.4

$$\text{Gas Yield (\%)} = \frac{\text{Product area x Gas product (\%)}}{\text{Total area}}$$

Equation 3.5

Chapter 4

Results and Discussion

4.1 Characterization of catalysts

The XRD patterns of calcined catalysts are shown in **Figure 2**. The broad peak in the range of 2Theta = 15-35° can be assign to amorphous SiO_2. Diffraction peaks at 28.2°, 31.5°, 38.5°, 50.1° and 59.8° correspond to monoclinic ZrO_2 (ICDD File No. 37-1484). The 2Theta at 25.3°, 36.9°, 37.7°, 38.5°, 48.0°, 53.8°, 55.0°, 62.1° and 62.7° indicated that TiO_2 is anatase phase [33]. After impregnation with Pt, a decrease in the intensity was observed. Otherwise, there were no changes in the crystalline structure of anatase after Pt loading. No diffraction peaks of Pt in the 0.5%Pt/TiO_2 were observed. This is probably attributed to the low Pt doping content (0.5%) as detected by ICP-OES (shown in Table 1) [34].

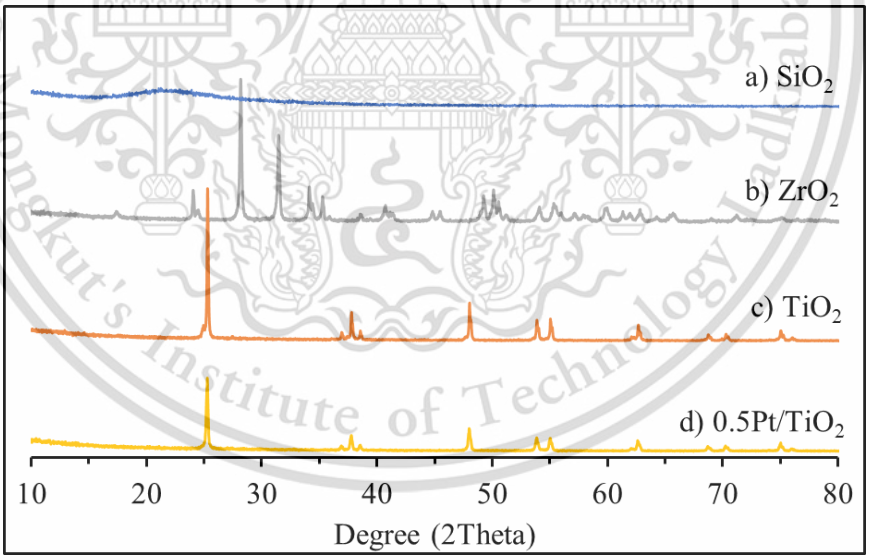

Figure 2 XRD patterns of calcined catalysts SiO_2, ZrO_2, TiO_2 and 0.5Pt/TiO_2.

Table 1 Specific surface area, platinum loading and platinum particle size of catalysts.

Entry	Catalyst	[a]S_{BET} (m^2/g)	[b]Pt content (wt.%)	[c]Pt particle size (nm)	[d]H_2 Consumption (mmol/g)
1	SiO_2	300.0	-	-	-
2	TiO_2	17.6	-	-	0.06
3	ZrO_2	5.5	-	-	-
4	0.5%Pt/SiO_2	280.1	0.4	15.9±6.3	-
5	0.5%Pt/TiO_2	10.6	0.4	6.0±3.0	0.05
6	0.5%Pt/ZrO_2	4.9	0.5	5.3±3.2	-

[a] Determined by N_2 adsorption/desorption

[b] Determined by ICP-OES

[c] Determined by TEM

[d] Determined by H_2-TPR

The specific surface area of platinum catalysts were slightly lower than their Pt-free counterparts due to the incorporated Pt species. SiO_2 has higher specific surface area than TiO_2 and ZrO_2. The Pt particles in 0.5Pt/SiO_2 are approximately 16 nm. While the Pt particles on TiO_2 (~6 nm) and ZrO_2 (~5 nm) are smaller than SiO_2 as shown in **Figure 3**.

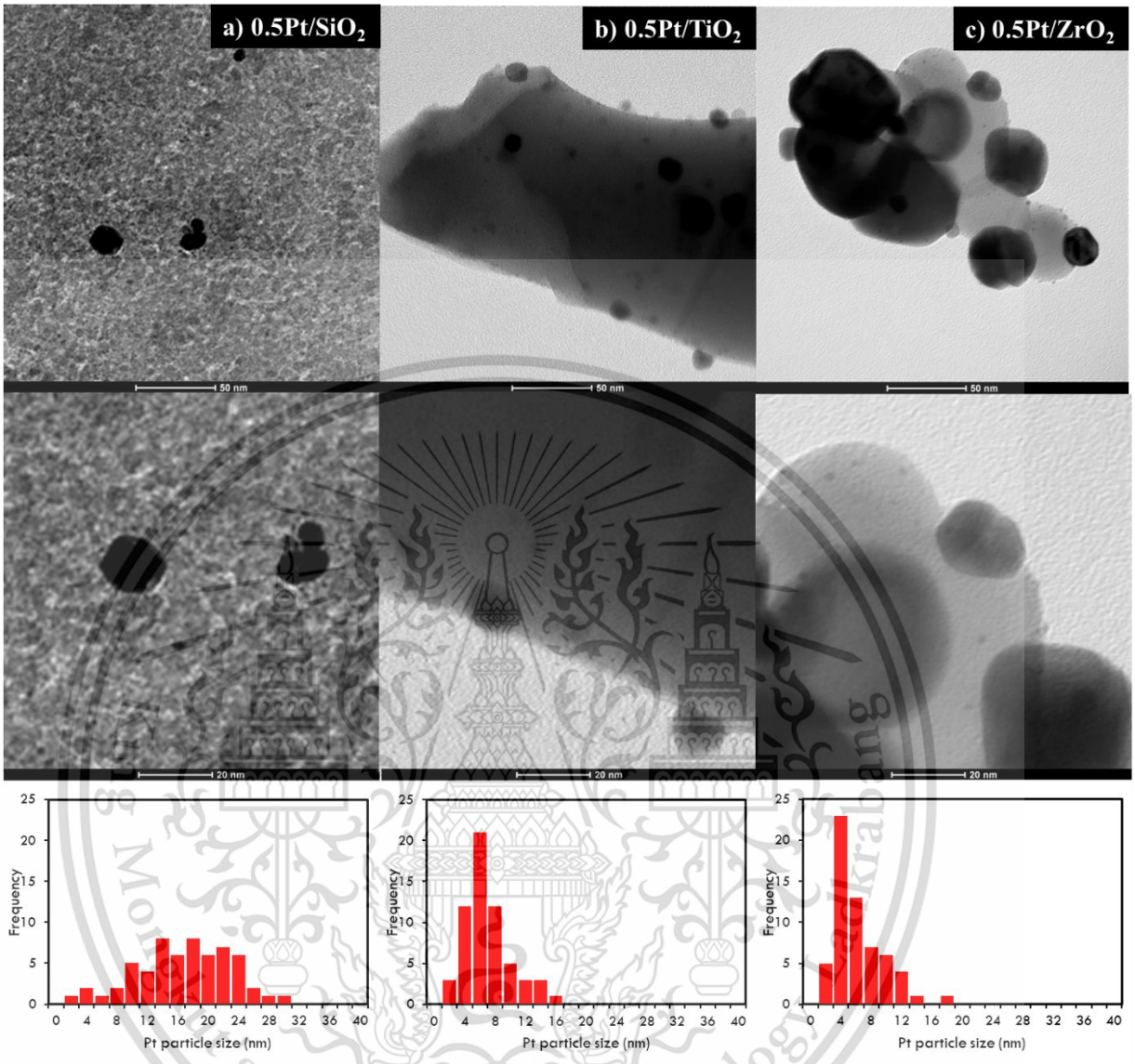

Figure 3 TEM images and size distributions of Pt particles on catalysts a) 0.5Pt/SiO_2, b) 0.5Pt/TiO_2, c) 0.5Pt/ZrO_2 (n=60 each).

The 0.5Pt/SiO_2 catalysts contain a wide range of Pt particle size between 2-30 nm. In addition, most Pt nanoparticles on TiO_2 and ZrO_2 were smaller than on SiO_2 even though SiO_2 has higher surface area than TiO_2 and ZrO_2. This is because the interaction between platinum with the reducible supports, i.e., TiO_2 and ZrO_2, were greater than that with the inert SiO_2 support. This can be observed by a decrease in reducing temperature of the TiO_2 support after platinum was incorporated as shown in **Figure 4**.

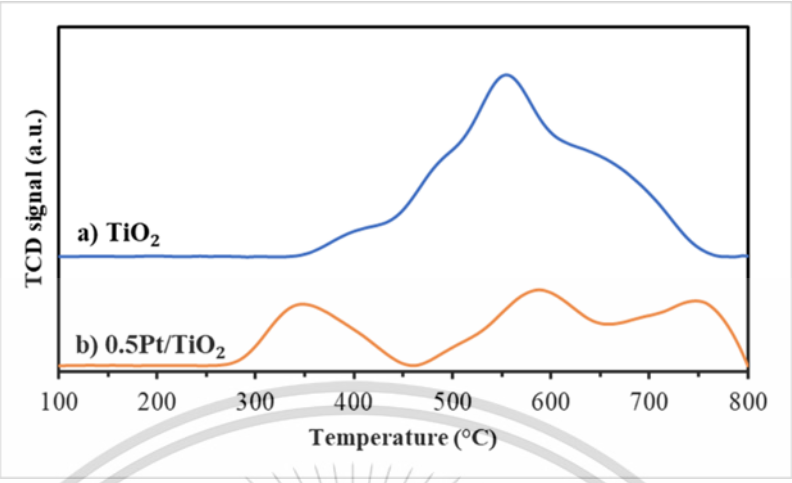

Figure 4 Temperature programmed reduction (H_2-TPR) profiles of a) TiO_2 and b) 0.5Pt/TiO_2.

It can be seen that TiO_2 show a hydrogen consumption at 550˚C which is the reduction of the surface oxygen of TiO_2 [35,36,37]. Meanwhile, 0.5Pt/TiO_2 exhibits additional H_2-consumption peak at 350˚C which could be attributed to the reduction of the TiO_2 facilitated by hydrogen spillover from Pt. This would result in oxygen vacancy on the TiO_2 surface that strongly interact with the Pt, so called the strong metal-support interaction (SMSI). However, the H_2-consumption of the samples with and without Pt are not much different (**Table1 entry 2 and 5**), presumably due to low loading of Pt (0.5%). Despite the same Pt loading as SiO_2, Pt sintering on TiO_2 and ZrO_2 would be inhibited during reduction. Accordingly, high dispersion and the presence of small Pt particle size (5-10 nm) can be observed by TEM for TiO_2 and ZrO_2 (**Figure 3**). It is worth noting that the Pt reduction peak was not observed because the decomposition of chloroplatinic precursor would have already resulted in the Pt form [38].

4.2 Reaction testing

4.2.1 Thermal steam cracking of *n*-hexane

Typically, in steam cracking processes, naphtha is fed into the convective section of a furnace for preheating and vaporization (450-600°C) and then radiant section (reaction zone) at 750-900°C. In this study, 750°C was chosen as the temperature at the reaction zone. As the steam cracking of naphtha is largely affected by temperature and residence time, the temperature profile configuration of the 3-zone reactor was first verified by different position of radiant section as shown in **Figure 5**.

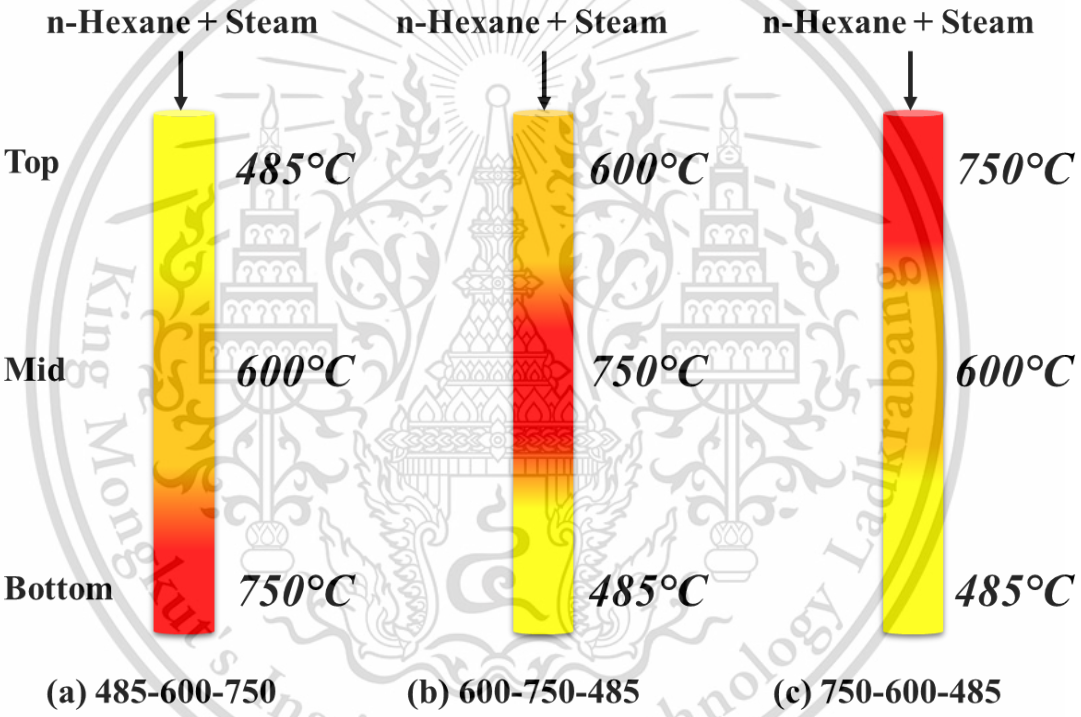

Figure 5 The 3-Zone reactor temperature profile (top-middle-bottom).

A higher conversion (88.6%) was obtained when reaction zone (750˚C) was located at the top of the reactor (**Figure 5c**). Meanwhile, lower conversion (80.8% and 81.5%) was obtained when the reaction zone was located at middle (**Figure 5b**) and bottom (**Figure 5a**) of the reactor. This is because, in addition to cracking at 750˚C, the remaining *n*-hexane can be further cracked and aromatized at 600˚C which located after the reaction zone. The main products, ethylene, from cracking at 750˚C can also further cracked and aromatized at this promoting zone (600˚C). This is supported by higher yields of methane

(11.3%) and C_6-C_8 (7.2%) as compared to those with other configurations (9.8% and 1.8%, respectively) as shown in **entry 1-3** of **Table 2**.

Table 2 The *n*-hexane conversion and yield of products in different temperature configuration.

Entry	Temperature pattern (°C)	LHSV, h^{-1} (Feed rate, ml/h)		Conversion (%)	Yield (%)					
					Ethylene	Propylene	Methane	Ethane	C_4-C_5	C_6-C_8
1	485-600-750	149 (8.1)		81.5	34.3	18.8	9.9	3.4	12.2	1.8
2	600-750-485	149 (8.1)		80.8	32.1	18.6	9.8	3.7	12.1	1.8
3	750-600-485	149 (8.1)		88.6	27.5	19.1	11.3	5.1	17.2	7.2
4	750-600-485	149 (8.1)	ZrO_2 @600°C	94.9	35.3	19.9	10.8	4.3	10.7	12.3
5	750-600-485	149 (8.1)	ZrO_2 @485°C	86.4	27.0	18.6	9.9	3.8	19.9	5.4

(Reaction condition; pressure: 1atm, *n*-hexane/steam ratio: 0.9, conversion and yield at 30 min)

When the configurations do not have promoting zone (**Table 2, entry 1-2**), further cracking does not occur as seen by higher ethylene yield but lower ethane, methane yield as compared to configuration with promoting zone (**Table 2, entry 3**). Although the preheating characteristics of 2 configurations are different (**Table 2, entry 1-2**), the conversion are the same. This finding suggests that the presence of a preheater in this study does not affect the reaction. Accordingly, the initial C-C bond dissociation cannot be promoted at the temperature below 600°C.

In another experiment, the inert bed was added to increase severity, especially in the promoting zone. High conversion and ethylene yield were obtained when ZrO_2 was added at 600°C. It is found that the C_4-C_5 products decreases, while the yields of benzene and C_6-C_8 increases as compared to thermal cracking. It can be concluded that cracking and aromatization reaction can be promoted by ZrO_2 at 600°C (**Table 2, entry 4**).

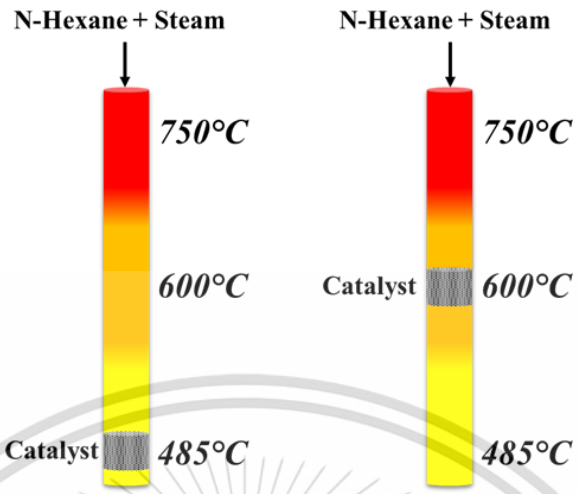

Figure 6 The position of catalysts in a 3-zone reactor.

To verify the effect of promoting zone (after the reaction zone at 750˚C) on cracking and aromatization, the steam cracking without and with a support should be compared by decreasing temperature of the promoting zone from 600˚C to 550˚C. It is found that the conversion was decreased from 88.6% (**Table 2, entry 3**) to 79.0% (**Table 3, entry 1**). This is because the severity in promoting zone decreases with temperature, resulting in lower cracking and aromatization. In a supporting manner, ethylene yield was decreased from 27.5% to 23.6%, and the trends for other cracked products are similar.

Table 3 The *n*-hexane conversion and yield of products over supports and various LHSV.

Entry	Temperature pattern (°C)	LHSV, h^{-1} (Feed rate, ml/h)		Conversion (%)	Yield (%)					
					Ethylene	Propylene	Methane	Ethane	C_4-C_5	C_6-C_8
1	750-550-485	149 (8.1)		79.0	23.6	17.2	8.3	3.2	21.6	4.3
2	750-550-485	268 (14.0)		61.4	23.5	14.6	7.3	3.4	11.3	0.7
3	750-550-485	317 (17.0)		50.9	17.4	12.0	5.3	3.1	10.6	0.5
4	750-550-485	149 (8.1)	ZrO_2 @550˚C	86.1	32.4	19.1	11.5	5.5	11.2	4.9
5	750-550-485	149 (8.1)	TiO_2 @550˚C	81.6	31.0	17.7	9.5	3.7	12.6	6.3
6	750-550-485	149 (8.1)	SiO_2 @550˚C	83.9	32.8	19.6	11.1	5.1	12.0	2.4

(Reaction condition; pressure: 1atm, *n*-hexane/steam ratio: 0.9, conversion and yield at 30 min)

In addition to temperature, the residence time affects the reaction activity, as seen from the decrease in conversion from 79.0% to 50.9% when LHSV was increased from 149 h^{-1} to 317 h^{-1} (**Table 3, entry 1-3**). This is because higher feed velocity (LHSV) decreases resident time for the feed in both reaction and promoting zone. Accordingly, the reaction severity is reduced resulting in less cracking and aromatization as seen from the lower yield of ethylene from 23.6% to 17.4% and C_6-C_8 yield from 4.3% to 0.5% (**Table 3, entry 1-3**).

In contrast, when supports were added into the promoting zone (**Table 3 entry 4-6**), the slight increase in the conversion (from ~79% to ~82-86%) and ethylene yield (from ~23% to ~31-33%) was observed due to the increase in reaction severity as discussed earlier. This is particularly emphasized for the ZrO_2 support (~86% conversion), because ZrO_2 possess some acid sites that may promote additional cracking. Meanwhile, TiO_2 and SiO_2 are relatively inert providing similar conversion (~82% and ~84%, respectively).

4.2.2 Catalytic steam cracking of *n*-hexane

As further cracking can be facilitated in the promoting zone, Pt catalysts were added in this zone to improve yields of light olefins. At higher LHSV (268 h^{-1}), the tandem system containing 0.5Pt/SiO_2 in promoting zone exhibited higher conversion (~69%) and ethylene yield (~24%) as compared to thermal cracking (~60% and ~22%) as shown in **Figure 7**. This is because Pt can promote C-C bond dissociative adsorption of *n*-hexane, thereby forming smaller alkylidene species on the surface. The adsorbed alkylidene species then undergoes C-C or C-H cracking to form smaller olefins (ethylene, propylene). Moreover, Pt can facilitate the C-H dissociation of *n*-hexane leading to the formation of olefins which can be aromatized as seen by the slight increase in C6-C8 yields.

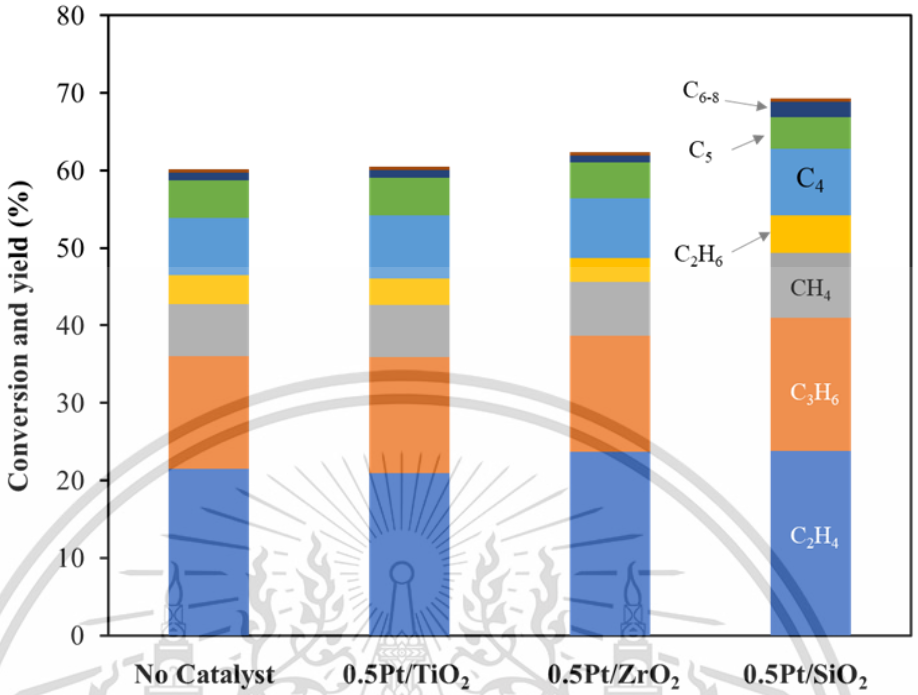

Figure 7 The *n*-hexane conversion and yield of products over platinum catalysts. (Reaction condition; Temperature: 750-550-485˚C, Packing Catalyst @550˚C, LHSV: 268 h^{-1}, pressure: 1 atm, *n*-hexane/steam ratio: 0.9, conversion and yield at 30 min)

The C-C bond dissociative adsorption on Pt surface usually requires at least 2 carbons atom on Pt terrace site (**Figure 8**). Thus, the Pt surface structure would affect the activity, so called "structure sensitive reaction". Since 0.5Pt/SiO_2 has relatively large Pt particle size as compared to 0.5Pt/TiO_2 and 0.5Pt/ZrO_2 (**Figure 3**), this catalyst would provide relatively more terrace sites that are effective for dissociative adsorption of hydrocarbon [39]. On the other hands, 0.5Pt/TiO_2 and 0.5Pt/ZrO_2 provide lower conversion (~60% and ~62%, respectively) as compared to 0.5Pt/SiO_2 (~69%). This is because both 0.5Pt/TiO_2 (~6 nm) and 0.5Pt/ZrO_2 (~5 nm) has smaller Pt particle size as compared to 0.5Pt/SiO_2 (~16 nm) as shown in **Figure 3**. The small Pt particle would provide less proportion of active terrace site but more under-coordinated surface atoms (step and kink) which are less active for dissociative adsorption of hydrocarbons [39].

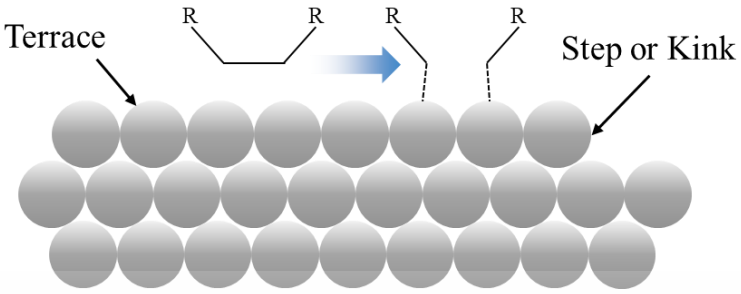

Figure 8 Dissociative adsorption of *n*-hexane on Pt surface.

The effect of Pt particle size on the observed activity can be supported by the tandem system containing 0.5Pt/TiO_2 with various particle size. It can be seen from **Figure 9** that the 0.5Pt/TiO_2 reduced under hydrogen for 14 h (Pt particle size ~10 nm) showed higher conversion (~57%), as compared to those reduced for 5 h (Pt particle size ~6 nm, conversion ~54%) and 1 h (Pt particle size ~5 nm, conversion ~53%). Ethylene, propylene, benzene and C6-C8 yields were also increased while C5 products were decreased. This again suggested that cracking and aromatization were promoted by large Pt particle size which was obtained from thermal sintering upon reduction at high temperature (600 °C) for long-time (14 h).

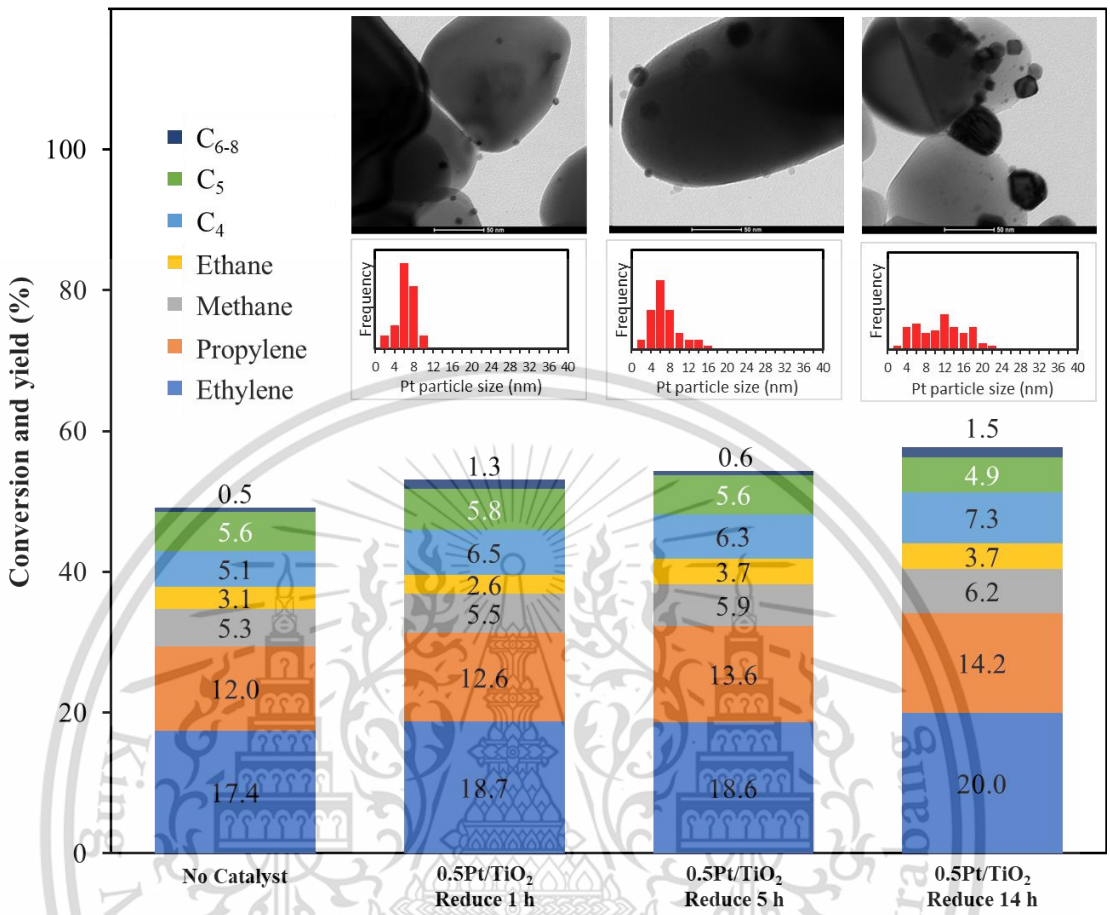

Figure 9 The *n*-hexane conversion and yield of products over 0.5Pt/TiO_2 at various reducing time.

(Reaction condition; Temperature: 750-550-485 °C, Packing Catalyst at 550°C, LHSV: 317 h^{-1}, pressure: 1 atm, *n*-hexane/steam ratio: 0.9, conversion and yield at 30 min)

The tandem system containing 0.5Pt/SiO_2 in the promoting zone provide high stability up to 6 h as seen from **Figure 10**. The insignificant decrease of *n*-hexane conversion over 0.5Pt/SiO_2 was observed from ~53% to ~52% after 360 min on stream. The system can provide steady production of ethylene and propylene with higher selectivity (~36% and ~24%) as compared to those for thermal steam cracking (~34% and ~23%).

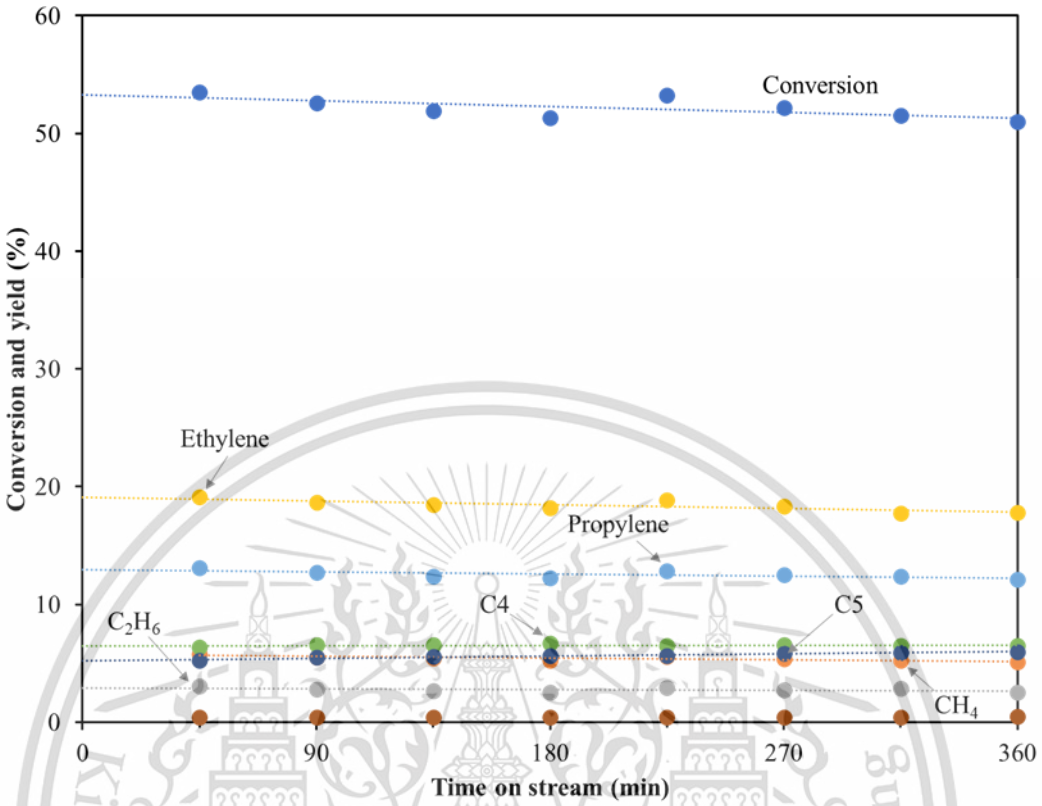

Figure 10 The *n*-hexane conversion and yield of products over 0.5%Pt/SiO_2.

Chapter 5

Conclusions and suggestions

5.1 Conclusions

The temperature configuration of the 3-zone furnace showed that high conversion was obtained when the reaction zone (750 ℃) was located at the top of reactor. This is because the unreacted *n*-hexane and the produced light olefins can be further cracked and aromatized at promoting zone (600 ℃) which locates after the reaction zone. It is found that conversion was decreased when the promoting zone temperature decreased from 600 ℃ to 550 ℃. This is because the severity in promoting zone decreased with temperature, resulting in lower secondary cracking and aromatization. The residence time also affects the reaction activity, and conversion was decreased when LHSV increased.

The olefins yield from n-Hexane catalytic steam cracking reaction could be enhance over Pt catalyst. The Pt/SiO_2 catalysts, which added into the promoting zone, provided higher conversion (~69%) and ethylene yield (~24%) as compared to thermal cracking (~60% and ~22%, respectively). This is because Pt can promote the C-C bond dissociative adsorption of *n*-hexane, thereby forming smaller alkylidene species on the surface which subsequently undergoes C-C or C-H cracking to form smaller olefins. Pt can also facilitate the C-H dissociation of *n*-hexane, leading to the formation olefins which can be aromatized to aromatic products. The Pt surface structure would affect the activity of the so called "structure sensitive reaction". The Pt/SiO_2 showed higher activity as compared to $0.5Pt/TiO_2$ and $0.5Pt/ZrO_2$ catalysts. This is because $0.5Pt/SiO_2$ has large Pt particle size with more terrace sites that are effective for dissociative adsorption of hydrocarbon. The effect of Pt particle size on the observed activity was also demonstrated by the catalytic activity of the $0.5Pt/TiO_2$ reduced for different durations. The $0.5Pt/TiO_2$ reduced under hydrogen for 14h showed high conversion as compared to those reduced for

5h and 1h. This result implies that cracking and aromatization were promoted by large Pt particle size which was obtained from thermal sintering upon reduction at high temperature for long time.

5.2 Suggestions

1. The effect of Pt loading over SiO_2 on *n*-hexane conversion could be further studied.

2. The variation of bi-metallic species over different supports on *n*-hexane conversion could be further evaluated.

3. The effect of contact time could be investigated, including the catalyst stability especially at longer time-on-stream, and regeneration.

References

[1] A. Corma, F.V. Melo, L. Sauvanaud, F. Ortega, (2005). Light cracked naphtha processing: controlling chemistry for maximum propylene production. pp 699-706. Catalysis Today

[2] Y.-K. Park, C.W. Lee, N.Y. Kang, W.C. Choi, S. Choi, S.H. Oh, D.S. Park, (2010). Catalytic cracking of lower-valued hydrocarbons for producing light olefins. pp 75-84. Catalysis Surveys from Asia 14 .

[3] H. Mochizuki, T. Yokoi, H. Imai, R. Watanabe, S. Namba, J.N. Kondo, T. Tatsumi, (2011). Facile control of crystallite size of ZSM-5 catalyst for cracking of hexane. pp 165-171. Microporous Mesoporous Mater. 145.

[4] T. Tago, H. Konno, M. Sakamoto, Y. Nakasaka, T. Masuda, (2011). Selective synthesis for light olefins from acetone over ZSM-5 zeolites with nano- and macro-crystal sizes. pp 183-191. Appl. Catal. A Gen. 403.

[5] H. Mochizuki, T. Yokoi, H. Imai, S. Namba, J.N. Kondo, T. Tatsumi, (2012). Effect of desilication of H-ZSM-5 by alkali treatment on catalytic performance in hexane cracking. pp 188-197. Appl. Catal. A Gen. 449.

[6] S. Inagaki, S. Shinoda, Y. Kaneko, K. Takechi, R. Komatsu, Y. Tsuboi, H. Yamazaki, J.N. Kondo, Y. Kubota, (2013). Facile fabrication of ZSM-5 zeolite catalyst with high durability to coke formation during catalytic cracking of paraffins. pp 74-78. ACS Catal. 3.

[7] H.S. Cerqueira, G. Caeiro, L. Costa, F.R. Ribeiro, (2008). Deactivation of FCC catalysts. pp 1-13. Journal of Molecular Catalysis A 292.

[8] D.T.Wickham, (2002). Methods for suppression of filamentous coke formation. US6 482 311B1,2002.

[9] Gary, James H.; Handwerk, Glenn E. (1993). Petroleum Refining Technology and Economics (Second ed.). Marcel Dekker. ISBN 0-8247-7150-8.

[10] Leffler, William L. (1985). Petroleum Refining for the Nontechnical Person (Second ed.). PennWell Books. ISBN 0-87814-280-0.

[11] Speight, James G. (2006). The Chemistry and Technology of Petroleum (Fourth ed.). CRC Press. ISBN 0-8493-9067-2.

[12] "Naphtha (petroleum), hydrotreated heavy". European Chemicals Agency.

[13] https://en.wikipedia.org/wiki/Petroleum_naphtha

[14] https://en.wikipedia.org/wiki/Hexane

[15] Kniel L, Winter O, Stork K (1980). Ethylene, keystone to the petrochemical industry. New York: M. Dekker. ISBN 978-0-8247-6914-7.

[16] "Ethylene Production and Manufacturing Process". Icis. Retrieved 2019-07-29.

[17] Amghizar I, Vandewalle LA, Van Geem KM, Marin GB (2017). "New Trends in Olefin Production". Engineering. 3 (2): 171–178. doi:10.1016/J.ENG.2017.02.006.

[18] Amghizar I, Vandewalle LA, Van Geem KM, Marin GB (2017). "New Trends in Olefin Production". Engineering. 3 (2): 171–178. doi:10.1016/J.ENG.2017.02.006.

[19] "Production: Growth is the Norm". Chemical and Engineering News. 84 (28): 59–236. July 10, 2006. doi:10.1021/cen-v084n034.p059.

[20] Propylene Production from Methanol. Intratec. 2012-05-31. ISBN 978-0-615-64811-8.

[21] https://en.wikipedia.org/wiki/Ethylene

[22] https://pubchem.ncbi.nlm.nih.gov/compound/Propene

[23] Ashford's Dictionary of Industrial Chemicals, Third edition, 2011, ISBN 978-0-9522674-3-0, pages 7766-9

[24] "Product Safety Assessment (PSA): Propylene". Dow Chemical Co. Archived from the original on 2013-06-22. Retrieved 2011-07-11.

[25] "Market Study: Propylene (2nd edition), Ceresana, December 2014". ceresana.com. Retrieved 2015-02-03.

[26] https://en.wikipedia.org/wiki/Propene

[27] Amghizar, Ismaël; Vandewalle, Laurien A.; Van Geem, Kevin M.; Marin, Guy B. (2017). "New Trends in Olefin Production". Engineering. 3 (2): 171–178. doi:10.1016/J.ENG.2017.02.006.

[28] Zimmermann, Heinz; Walzl, Roland (2009). Ullmann's Encyclopedia of Industrial Chemistry. Weinheim: Wiley-VCH. doi:10.1002/14356007.a10_045.pub3.

[29] https://en.wikipedia.org/wiki/Steam_cracking

[30] S.M. Babitz et al. / Applied Catalysis A: General 179 (1999) 71-86

[31] A. Yamaguchi et al. / Fuel Processing Technology 126 (2014) 343–349

[32] Sungwon Lee et al. (2016). “Effect of Particle Size upon Pt/SiO2 Catalytic Cracking of n -Dodecane under Supercritical Conditions: In situ SAXS and XANES Studies”. ChemCatChem Volume 9, Issue 1 p. 99-102

[33] T. Thirugnanasambandan, A. Marimuthu, Titanium dioxide (TiO2) Nanoparticles – XRD Analyses – An Insight

[34] Mohammad W. Kadi, R.M. Mohamed, (2013). Enhance Photocatalytic Activity of ZrO_2-SiO_2 Nanoparticles by Platinum Doping. International Journal of Photoenergy.

[35] X.Y. Jiang, G.H. Ding, L.P. Lou, Y.X. Chen, X.M. Zheng, J. Mol. Catal. A: Chem. 218 (2004) 187.

[36] J.A. Wang, A. Cuan, J. Salmones, N. Nava, S. Castillo, M. Mora´n-Pineda, F. Rojas, Appl. Surf. Sci. 230 (2004) 94.

[37] N.S. de Resende, J.-G. Eon, M. Schmal, J. Catal. 183 (1999) 6.

[38] https://www.researchgate.net/publication/305634230_The_Effect_of_Metal_Type_on_Hydrodeoxygenation_of_Phenol_Over_Silica_Supported_Catalysts

[39] Siwen Wang et al. / Phys. Chem. Chem. Phys., (2018), 20, 6055-6059

APPENDICES

APPENDIX A

CALCULATION

A1. Liquid hour space velocity, LHSV

$$\text{LHSV} = \frac{\text{Feed rate (ml/h)}}{\text{Volume (ml)}}$$

Calculation example.

In the reaction using 14.0 mL/h of *n*-hexane and 10.1 ml/h of water in feed the reaction volume is calculated from cylinder area inside quartz tube ($\pi(0.03\text{cm})^2(32\text{cm})$)

$$\text{LHSV} = \frac{(14.0+10.1)(\text{ml/h})}{(22/7)(0.03\text{cm})(0.03\text{cm})(32\text{cm})}$$

$$= 268\ h^{-1}$$

A2. Calculation of % yield of products

The coke deposit on catalysts was determined by weighing the quartz reactor (including catalyst and packings) before and after reaction. The different weight was use for calculating the coke product as follows:

$$\text{Solid product, coke } (\%\text{wt.}) = \frac{[\text{Tube after run (g) - Tube before run (g)}]\times 100}{\text{Feed per run (g)}}$$

For example;

$$\text{Solid product, coke } (\%\text{wt.}) = \frac{[37.0123\text{-}36.8133]\times 100}{18.5693\ \text{g}} = 1.07\ \%$$

The condensed liquid products were determined by adding cyclohexane 1.00ml as internal standard, then adjust to 50ml with dodecane. Then product solution is

analyzed by gas chromatograph (GC-FID). The products are recorded as a chromatogram and peak area are measured and calculated. Compared with retention time, internal standard peak areas, the species and composition of each product will be determined in equation below:

$$\text{Liquid product (g)} = \frac{\left(\frac{\text{Product area in sample}}{\text{Cyclohexane area in sample}}\right)}{\left(\frac{\text{Product area in standard}}{\text{Cyclohexane area in standard}}\right)} \text{x Product weight in standard (g)}$$

For example;

$$\text{Benzene product (g)} = \frac{\left[\frac{9292.0}{10333.0}\right]}{\left[\frac{3926.0}{5267.7}\right]} \text{ x } 0.44 \text{ g} = 0.53 \text{ g}$$

Non-condensed gas products were analyzed on-line by a gas chromatograph.

Table A1 The summation of the peak area of non-condensed gas products

Product	Peak area
Methane	188142
Ethane	78732
Ethylene	508462
Propane	9355
Propylene	366646
i-Butane	287
n-Butane	978
Propadiene	4125
trans-2-Butene	7177
1-Butene	58558
i-Butylene	23672
cis-2-Butene	6155

i-Pentane	384
n-Pentane	550
1,3-Butadiene	41127
C_5 Olefins	21151
C_{6+}	21568
n-Hexane (Feed)	12905
Total	1349974

*Information of ethanol conversion over ZrO_2 @485°C, time on stream: 30 minutes, Pressure: 1 atm, feed rate of H_2O: 5.89 mL/h, n-hexane: 8.1mL/h, LHSV: 149h^{-1}

Calculate the percent gas yield of each component in sample as follows:

$$\%\text{Gas product} = 100 - \%\text{Solid Product} - \%\text{Liquid Product}$$

$$\%\text{Gas yield} = \frac{\text{Product area}}{\text{Total area}} \times \text{Gas product}$$

For example;

$$\%\text{Gas product} = 100 - 1.07 - 20.60 = 78.32\%$$

$$\%\text{Ethylene yield} = \frac{508462 \times 78.32\%}{1349974} = 29.50$$

The percent yield of each product obtained from above calculation is shown in **Table A2.**

Table A2 Yield of product derived from normalization method.

Time on stream (min)	**30**
Conversion (%)	89.46
Yield of product (%)	
Methane	10.92
Ethane	4.57

Ethylene	29.50
Propane	0.54
Propylene	21.27
Unknown 1	0.24
Butane	0.07
C_4 olefins	5.54
Butadiene	2.39
C_5 olefins	7.90
C_{6+}	5.45
Coke	1.07

A3. Conversion

%Conversion can be calculated from the following equation:

$$\%\text{Conversion} = 100 - \%\text{hexane yield in Liquid} - \%\text{hexane yield in Gas}$$

A4. Selectivity

%Selectivity can be obtained from the following equation:

$$\%\text{Selectivity of each product} = \frac{\%\text{Yield of each product} \times 100}{\%\text{Conversion}}$$

For example;

$$\%\text{Selectivity of Ethylene} = \frac{29.50 \times 100}{89.46} = 32.98$$

APPENDIX B

GAS CHROMATOGRAM

Analysis of gas product from gas chromatography

Prior to analysis, each product in the sample was identified the by GC-MS (gas chromatography with mass spectrometer detector). Then, the quantitative analysis of each product was carried out by GC-FID (gas chromatography with flame ionization detector) with the condition expressed in **Table B1** for the non-condensed gas sample, and **Table B2** for the liquid sample. The chromatogram of gas products was identified using reference standard as shown in **Figure B1** for the non-condensed gas sample, and **Figure B2** for the liquid sample.

Table B1 The GC condition for quantitative analysis (for non-condensed gas products)

Column	HP-PLOT, 30 m x 0.53 mm x 15 µm
Temperature program	35°C (1.5 min hold) to 100°C at 5°C/min to 180°C at 10°C/min (5.5 min hold)
Carrier gas	Nitrogen at 3.05 mL/min
Injection	250°C
Detector	FID at 250°C

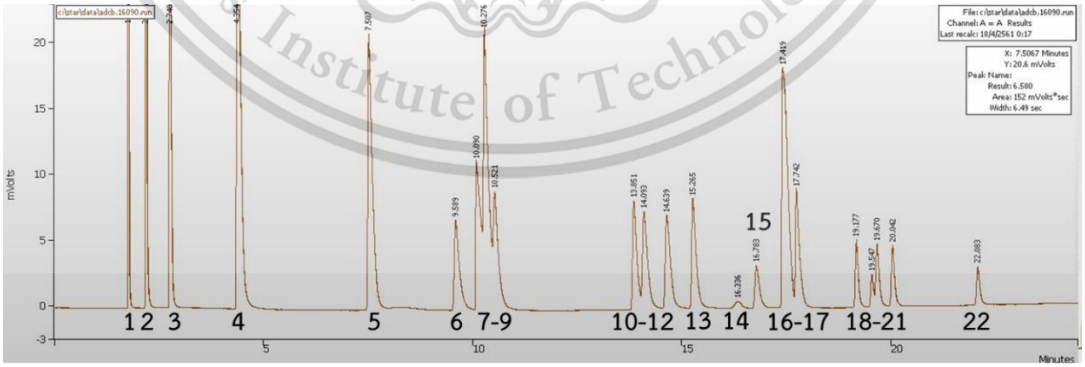

Figure B1 Chromatogram of hydrocarbon gas standard.

1. Methane
2. Ethane
9. Acetylene
10. trans-2-Butene
17. Propyne
18. trans-2-Pentene

3. Ethylene	11. 1-Butene	19. 2-Methyl-2-butene
4. Propane	12. iso-Butylene	20. 1-Pentene
5. Propylene	13. cis-2-Butene	21. cis-2-Pentene
6. iso-Butane	14. iso-Pentane	22. *n*-Hexane
7. n-Butane	15. *n*-Pentane	
8. Propadiene	16. 1,3-Butadiene	

Table B2 The GC condition for quantitative analysis (for liquid products)

Column	MXT-1, 60 m x 0.25 mm x 0.5 μm
Temperature program	40°C (5 min hold) to 280°C at 15°C/min (2 min hold)
Carrier gas	Nitrogen
Split ratio	50:1
Injection	250°C
Detector	FID at 250°C

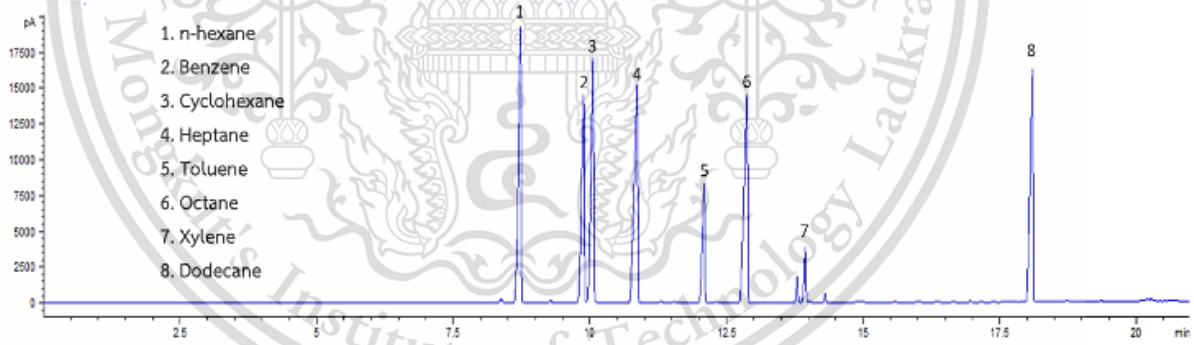

Figure B2 Chromatogram of hydrocarbon liquid standard.

Table B3 The raw data of hydrocarbon liquid standard.

Heavy HC, MXT-1								
Standard								
Name	bp (°C)	v (ml)	d (g/ml)	weight (g)	RT (min)	Area	Area ratio	
n-Hexane	68	0.5	0.66	0.33		1906.2	0.36	
Benzene	80.1	0.5	0.88	0.44		3926	0.75	
Cyclohexane	80.7	1.0	0.78	0.78		5267.7	1.00	4.11
n-Heptane	98.4	0.5	0.68	0.34		3030.7	0.58	
Toluene	110.6	0.5	0.87	0.43		4144.4	0.79	
n-Octane	125	0.5	0.70	0.35		3462 .1	0.66	
Ethylbenzene	136	0.5	0.87	0.43		5269.1	1.00	
Xylene	138-144	0.5	0.86	0.43		3054.8	0.58	
Dodecane	216.3	20.5	0.75	15.38		101572	19.28	
Total		25.0				128171		

APPENDIX C

CATALYTIC ACTIVITY DATA

C1. The *n*-hexane conversion and yield of at temperature pattern 485-600-750°C

Table C1 The *n*-hexane conversion and yield of steam thermal cracking

Time on stream (min)	30	75	120	165	210
Conversion (%)	85.01	83.36	80.93	77.07	77.97
Yield of product (%)					
Methane	10.76	9.96	9.95	10.17	9.93
Ethane	4.16	3.60	3.26	3.15	2.97
Ethylene	37.15	34.55	34.62	34.78	34.42
Propane	0.51	0.49	0.46	0.44	0.43
Propylene	22.97	20.66	18.46	17.47	16.73
Unknown	0.13	0.20	0.28	0.30	0.33
Butane	0.12	0.19	0.22	0.19	0.20
C_4 olefins	5.37	7.75	6.42	5.42	4.77
Butadiene	1.64	3.30	3.72	4.08	4.20
C_5 olefins	0.37	0.89	1.58	1.67	1.70
C_{6+}	1.62	1.58	1.79	1.81	2.12
Coke	0.19	0.19	0.19	0.19	0.19

(Reaction condition; Pressure: 1 atm, feed rate of H_2O: 5.89 mL/h, *n*-hexane: 8.1mL/h, LHSV: 149h^{-1})

C2. The *n*-hexane conversion and yield of at temperature pattern 600-750-485°C

Table C2 The *n*-hexane conversion and yield of steam thermal cracking

Time on stream (min)	**30**	**75**	**120**	**165**
Conversion (%)	84.46	82.22	79.13	77.07
Yield of product (%)				
Methane	11.32	9.86	9.68	9.16
Ethane	4.61	3.80	3.56	3.11
Ethylene	34.72	33.05	32.15	31.51
Propane	0.51	0.48	0.45	0.42
Propylene	21.29	19.73	17.88	17.24
Unknown	0.17	0.19	0.22	0.22
Butane	0.14	0.19	0.18	0.18
C_4 olefins	5.39	6.67	5.79	5.62
Butadiene	2.61	3.81	4.09	4.09
C_5 olefins	0.43	1.03	1.33	1.42
C_{6+}	1.41	1.53	1.92	2.22
Coke	1.88	1.88	1.88	1.88

(Reaction condition; Pressure: 1 atm, feed rate of H_2O: 5.89 mL/h, *n*-hexane: 8.1mL/h, LHSV: 149h^{-1})

C3. The *n*-hexane conversion and yield of at temperature pattern 750-600-485°C

Table C3 The *n*-hexane conversion and yield of steam thermal cracking

Time on stream (min)	**30**	**75**	**120**	**165**	**210**
Conversion (%)	91.38	89.68	87.76	86.55	86.20
Yield of product (%)					
Methane	12.82	12.41	11.91	11.71	10.96
Ethane	6.20	5.83	5.40	5.18	4.47
Ethylene	31.11	29.32	28.60	28.15	28.78
Propane	0.69	0.64	0.60	0.57	0.53
Propylene	23.43	20.76	19.74	18.88	18.89
Unknown	0.23	0.24	0.16	0.16	0.18
Butane	0.09	0.12	0.18	0.18	0.18
C_4 olefins	6.12	7.02	6.45	6.06	5.98
Butadiene	2.87	3.89	4.01	3.98	3.98
C_5 olefins	1.06	2.28	3.29	3.58	3.62
C_{6+}	6.45	6.87	7.09	7.79	8.31
Coke	0.32	0.32	0.32	0.32	0.32

(Reaction condition; Pressure: 1 atm, feed rate of H_2O: 5.89 mL/h, *n*-hexane: 8.1mL/h, LHSV: 149h^{-1})

C4. The *n*-hexane conversion and yield of at temperature pattern 750-600-485°C over ZrO_2 catalyst

Table C4 The *n*-hexane conversion and yield of over ZrO_2 at 600°C

Time on stream (min)	30	75	120	165	210
Conversion (%)	97.38	96.27	94.87	93.80	92.21
Yield of product (%)					
Methane	12.20	10.94	10.33	10.55	9.99
Ethane	5.52	4.38	3.85	4.05	3.47
Ethylene	36.51	35.80	35.16	34.49	34.56
Propane	0.62	0.54	0.51	0.50	0.48
Propylene	20.92	20.47	19.84	19.33	18.78
Unknown 1	0.19	0.20	0.20	0.20	0.23
Butane	0.15	0.18	0.18	0.19	0.18
C_4 olefins	4.63	5.96	6.06	6.04	5.86
Butadiene	3.60	4.08	3.69	3.76	3.77
C_5 olefins	0.47	0.87	1.48	1.56	1.62
C_{6+}	11.77	12.04	12.79	12.34	12.48
Coke	0.79	0.79	0.79	0.79	0.79

(Reaction condition; Packing ZrO_2 @600°C, Pressure: 1 atm, feed rate of H_2O: 5.89 mL/h, *n*-hexane: 8.1mL/h, LHSV: 149h^{-1})

Table C5 The *n*-hexane conversion and yield of over ZrO_2 at 485°C

Time on stream (min)	30	75	120	165	210
Conversion (%)	89.46	87.80	85.84	84.28	84.76
Yield of product (%)					
Methane	10.92	10.27	9.88	9.54	9.11
Ethane	4.57	3.96	3.73	3.45	3.25
Ethylene	29.50	28.01	26.59	25.59	25.42
Propane	0.54	0.48	0.45	0.42	0.41
Propylene	21.27	19.44	18.17	17.20	16.89
Unknown 1	0.24	0.12	0.12	0.12	0.12
Butane	0.07	0.10	0.09	0.09	0.08
C_4 olefins	5.54	7.29	6.91	6.57	6.34
Butadiene	2.39	3.44	3.61	3.66	3.63
C_5 olefins	7.90	9.06	10.13	10.86	12.31
C_{6+}	5.45	4.56	5.08	5.72	6.13
Coke	1.07	1.07	1.07	1.07	1.07

(Reaction condition; Packing ZrO_2 @485°C, Pressure: 1 atm, feed rate of H_2O: 5.89 mL/h, *n*-hexane: 8.1mL/h, LHSV: 149h^{-1})

C5 The *n*-hexane conversion and yield of at temperature pattern 750-550-485°C

Table C6 The *n*-hexane conversion and yield of steam thermal cracking at LHSV 149 h^{-1}

Time on stream (min)	**30**	**75**	**120**	**165**	**210**
Conversion (%)	82.00	80.63	79.00	77.25	75.82
Yield of product (%)					
Methane	9.25	8.87	8.32	7.77	7.32
Ethane	3.85	3.65	3.24	2.75	2.54
Ethylene	26.57	23.81	23.30	22.65	22.01
Propane	0.46	0.42	0.39	0.36	0.34
Propylene	20.22	18.12	16.76	15.94	15.22
Unknown	0.12	0.13	0.23	0.27	0.25
Butane	0.15	0.11	0.08	0.08	0.07
C_4 olefins	5.85	7.68	7.20	6.87	6.48
Butadiene	2.25	3.08	3.35	3.32	3.35
C_5 olefins	9.29	10.67	11.89	12.75	13.57
C_{6+}	4.00	4.11	4.24	4.48	4.68
Coke	0.00	0.00	0.00	0.00	

(Reaction condition; Pressure: 1 atm, feed rate of H_2O: 5.89 mL/h, *n*-hexane: 8.1mL/h, LHSV: 149h^{-1})

Table C7 The *n*-hexane conversion and yield of steam thermal cracking at LHSV 268 h^{-1}

Time on stream (min)	**45**	**90**	**135**	**180**	**225**	**270**	**315**	**360**
Conversion (%)	61.4	59.90	58.99	58.38	59.64	58.41	57.47	56.89
Yield of product (%)								
Methane	7.33	7.15	6.63	6.45	6.83	6.34	6.30	6.25
Ethane	3.44	3.37	2.85	2.64	3.07	2.45	2.71	2.60
Ethylene	23.56	22.22	22.49	22.45	23.53	22.64	22.08	21.65
Propane	0.37	0.36	0.34	0.33	0.36	0.32	0.33	0.32
Propylene	14.65	14.19	14.06	13.84	14.14	13.80	13.44	13.31
Unknown	0.00	0.00	0.00	0.00	0.00	0.00	0.00	0.00
Butane	0.16	0.15	0.14	0.14	0.14	0.12	0.14	0.14
C_4 olefins	4.86	5.35	5.32	4.18	4.18	5.26	4.79	4.91
Butadiene	1.81	1.61	1.59	1.67	1.67	1.53	1.61	1.59
C_5 olefins	4.49	4.75	4.81	4.80	4.80	5.03	5.13	5.17
C_{6+}	0.74	0.75	0.77	0.91	0.91	0.93	0.94	0.96
Coke	0.00	0.00	0.00	0.00	0.00	0.00	0.00	0.00

(Reaction condition; Pressure: 1 atm, feed rate of H_2O: 10.2mL/h, *n*-hexane: 14.0mL/h, LHSV: 268h^{-1})

Table C8 The *n*-hexane conversion and yield of steam thermal cracking at LHSV 317 h^{-1}

Time on stream (min)	**45**	**90**	**135**	**180**
Conversion (%)	52.55	51.92	51.31	50.77
Yield of product (%)				
Methane	5.49	5.30	5.87	5.11
Ethane	3.03	2.50	3.21	2.66
Ethylene	18.67	18.80	17.52	17.90
Propane	0.37	0.34	0.36	0.35
Propylene	12.72	12.39	11.90	12.04
Unknown	0.00	0.00	0.00	0.00
Butane	0.10	0.14	0.15	0.15
C_4 olefins	5.37	5.43	5.03	5.07
Butadiene	0.81	0.87	1.02	1.17
C_5 olefins	5.01	5.19	5.27	5.32
C_{6+}	0.98	0.98	0.98	1.01
Coke	0.00	0.00	0.00	0.00

(Reaction condition; Pressure: 1 atm, feed rate of H_2O: 13.1mL/h, *n*-hexane: 18.0mL/h, LHSV: 317h^{-1})

C6 The *n*-hexane conversion and yield of at temperature pattern 750-550-485°C

Table C9 The *n*-hexane conversion and yield over ZrO_2 at LHSV 149 h^{-1}

Time on stream (min)	**30**	**75**	**120**	**165**	**210**
Conversion (%)	88.95	87.36	86.00	84.60	83.47
Yield of product (%)					
Methane	11.36	11.36	11.58	11.76	11.60
Ethane	5.91	5.74	5.50	5.37	5.19
Ethylene	33.35	31.77	32.05	32.39	32.21
Propane	0.61	0.59	0.57	0.55	0.53
Propylene	21.95	19.92	18.65	17.85	17.29
Unknown	0.12	0.14	0.16	0.00	0.00
Butane	0.14	0.16	0.17	0.00	0.15
C_4 olefins	5.61	5.69	4.77	3.92	3.79
Butadiene	2.71	3.61	3.54	4.03	3.70
C_5 olefins	2.34	2.80	3.36	3.10	3.19
C_{6+}	4.22	4.96	5.04	5.00	5.18
Coke	0.62	0.62	0.62	0.62	0.62

(Reaction condition; Packing ZrO_2 @550°C, Pressure: 1 atm, feed rate of H_2O: 5.89 mL/h, *n*-hexane: 8.1mL/h, LHSV: 149h^{-1})

Table C10 The *n*-hexane conversion and yield over TiO_2 at LHSV 149 h^{-1}

Time on stream (min)	**30**	**75**	**120**	**165**	**210**
Conversion (%)	N/A	83.12	81.51	80.05	79.12
Yield of product (%)					
Methane		9.62	9.51	9.37	9.35
Ethane		3.83	3.60	3.61	3.59
Ethylene		31.49	31.10	30.46	29.92
Propane		0.47	0.45	0.45	0.44
Propylene		18.43	17.53	17.03	16.64
Unknown		0.17	0.19	0.18	0.18
Butane		0.17	0.16	0.16	0.16
C_4 olefins		6.01	5.31	4.93	4.76
Butadiene		3.42	3.70	3.72	3.32
C_5 olefins		3.41	3.65	3.72	4.20
C_{6+}		6.09	6.30	6.41	6.55
Coke		0.00	0.00	0.00	0.00

(Reaction condition; Packing TiO_2 @550°C, Pressure: 1 atm, feed rate of H_2O: 5.89 mL/h, *n*-hexane: 8.1mL/h, LHSV: 149h^{-1})

Table C11 The *n*-hexane conversion and yield over SiO_2 at LHSV 149 h^{-1}

Time on stream (min)	**30**	**75**	**120**	**165**	**210**
Conversion (%)	85.39	84.81	83.89	83.14	82.52
Yield of product (%)					
Methane	11.47	11.14	11.25	10.66	11.06
Ethane	6.3	5.47	5.08	4.20	4.58
Ethylene	33.38	32.27	32.67	33.23	32.24
Propane	0.62	0.58	0.55	0.51	0.50
Propylene	22.16	20.06	18.93	18.79	18.25
Unknown	0.10	0.14	0.17	0.19	0.19
Butane	0.11	0.16	0.17	0.17	0.17
C_4 olefins	3.95	5.68	5.09	5.14	5.13
Butadiene	1.79	3.25	3.74	3.80	3.83
C_5 olefins	3.23	3.64	3.88	3.99	4.06
C_{6+}	2.26	2.40	2.37	2.46	2.52
Coke	0.00	0.00	0.00	0.00	0.00

(Reaction condition; Packing SiO_2 @550°C, Pressure: 1 atm, feed rate of H_2O: 5.89 mL/h, *n*-hexane: 8.1mL/h, LHSV: 149h^{-1})

Table C12 The *n*-hexane conversion and yield over 0.5Pt/TiO_2 at LHSV 268 h^{-1}

Time on stream (min)	**45**	**90**	**135**	**180**
Conversion (%)	62.65	60.90	59.52	58.73
Yield of product (%)				
Methane	7.41	6.69	6.41	6.23
Ethane	3.96	3.52	3.26	2.96
Ethylene	21.43	20.57	20.75	21.20
Propane	0.41	0.38	0.37	0.34
Propylene	15.83	14.74	14.84	14.44
Unknown	0.03	0.04	0.04	0.04
Butane	0.08	0.08	0.08	0.07
C_4 olefins	6.21	7.38	6.17	5.98
Butadiene	1.75	1.67	1.65	1.57
C_5 olefins	4.54	4.78	4.89	4.84
C_{6+}	1.00	1.05	1.05	1.05
Coke	0.00	0.00	0.00	0.00

(Reaction condition; Packing 0.5Pt/TiO_2 @550°C, Pressure: 1 atm, feed rate of H_2O: 10.2 mL/h, *n*-hexane: 14.0mL/h, LHSV: 268h^{-1})

Table C13 The *n*-hexane conversion and yield over 0.5Pt/ZrO_2 at LHSV 268 h^{-1}

Time on stream (min)	**45**	**90**	**135**	**180**
Conversion (%)	60.46	59.08	58.06	57.20
Yield of product (%)				
Methane	6.87	6.52	6.41	6.17
Ethane	3.12	2.78	2.68	2.63
Ethylene	23.28	22.68	22.28	21.81
Propane	0.35	0.34	0.33	0.32
Propylene	14.79	14.28	13.91	13.78
Unknown	0.07	0.07	0.07	0.07
Butane	0.06	0.06	0.06	0.06
C_4 olefins	5.65	5.84	5.76	5.77
Butadiene	1.60	1.49	1.43	1.451
C_5 olefins	3.98	4.29	4.40	4.45
C_{6+}	0.69	0.71	0.72	0.73
Coke	0.00	0.00	0.00	0.00

(Reaction condition; Packing 0.5Pt/ZrO_2 @550°C, Pressure: 1 atm, feed rate of H_2O: 10.2 mL/h, *n*-hexane: 14.0mL/h, LHSV: 268h^{-1})

Table C14 The *n*-hexane conversion and yield over 0.5Pt/SiO_2 at LHSV 268 h^{-1}

Time on stream (min)	45	90	135	180	225	270	315	360
Conversion (%)	72.17	69.77	68.16	67.26	68.18	66.26	64.99	63.87
Yield of product (%)								
Methane	9.08	8.63	7.87	7.94	8.04	7.77	7.50	7.31
Ethane	5.69	5.36	3.87	4.33	4.58	4.04	3.95	3.71
Ethylene	24.01	23.78	23.84	23.50	24.37	23.50	23.31	22.73
Propane	0.59	0.54	0.43	0.44	0.51	0.44	0.41	0.41
Propylene	18.10	17.28	17.14	16.43	17.33	16.37	15.99	15.75
Unknown	0.03	0.04	0.04	0.04	0.05	0.05	0.05	0.05
Butane	0.10	0.09	0.09	0.08	0.09	0.08	0.08	0.08
C_4 olefins	5.89	5.69	6.82	6.41	5.56	6.13	6.09	6.23
Butadiene	2.71	2.42	2.16	1.94	2.50	0.21	1.95	1.89
C_5 olefins	3.64	4.07	4.27	4.33	3.81	6.28	4.26	4.32
C_{6+}	2.34	1.87	1.60	1.86	1.34	1.39	1.40	1.41
Coke	0.00	0.00	0.00	0.00	0.00	0.00	0.00	0.00

(Reaction condition; Packing 0.5Pt/SiO_2 @550°C, Pressure: 1 atm, feed rate of H_2O: 10.2 mL/h, *n*-hexane: 14.0mL/h, LHSV: 268h^{-1})

C6 The *n*-hexane conversion and yield of over 0.5Pt/TiO_2 (with different reducing time) at temperature pattern 750-550-485°C

Table C14 The *n*-hexane conversion and yield over 0.5Pt/TiO_2 reduced 1h at LHSV 317 h^{-1}

Time on stream (min)	45	90	135	180	225	270	315	360
Conversion (%)	54.57	53.38	52.03	50.93	51.97	50.62	49.81	49.15
Yield of product (%)								
Methane	7.52	5.53	6.61	5.15	6.23	5.17	6.12	5.15
Ethane	2.95	2.65	3.22	2.55	3.15	2.65	2.92	2.51
Ethylene	21.25	18.71	17.52	17.46	18.18	17.53	17.18	17.08
Propane	0.28	0.31	0.29	0.29	0.31	0.31	0.28	0.29
Propylene	12.36	12.60	11.29	11.92	11.90	12.13	11.02	11.53
Unknown	0.00	0.00	0.00	0.00	0.00	0.00	0.00	0.00
Butane	0.06	0.10	0.11	0.10	0.10	0.10	0.10	0.10
C_4 olefins	2.27	5.04	4.57	4.90	4.89	5.15	4.74	4.83
Butadiene	1.30	1.31	1.24	1.25	0.95	1.10	0.93	1.08
C_5 olefins	5.30	5.83	6.03	6.15	5.63	5.86	5.88	5.95
C_{6+}	1.27	1.29	1.15	1.17	0.60	0.63	0.63	0.64
Coke	0.00	0.00	0.00	0.00	0.00	0.00	0.00	0.00

(Reaction condition; Packing 0.5Pt/TiO_2 @550°C, Pressure: 1 atm, feed rate of H_2O: 13.1 mL/h, *n*-hexane: 18.0mL/h, LHSV: 268h^{-1})

Table C15 The *n*-hexane conversion and yield over 0.5Pt/TiO_2 reduced 5h at LHSV 317 h^{-1}

Time on stream (min)	**45**	**90**	**135**	**180**
Conversion (%)	56.26	55.02	54.25	53.59
Yield of product (%)				
Methane	5.93	5.60	5.64	5.46
Ethane	3.72	3.31	3.26	3.29
Ethylene	18.64	18.26	17.91	17.50
Propane	0.38	0.36	0.34	0.35
Propylene	13.62	12.99	12.56	12.44
Unknown	0.04	0.05	0.06	0.06
Butane	0.06	0.06	0.06	0.06
C_4 olefins	5.33	5.38	5.27	5.08
Butadiene	0.89	1.09	1.14	1.28
C_5 olefins	5.56	5.81	5.89	5.93
C_{6+}	0.58	0.60	0.61	0.63
Coke	1.51	1.51	1.51	1.51

(Reaction condition; Packing 0.5Pt/TiO_2 @550°C, Pressure: 1 atm, feed rate of H_2O: 13.1 mL/h, *n*-hexane: 18.0mL/h, LHSV: 268h^{-1})

Table C16 The *n*-hexane conversion and yield over 0.5Pt/TiO_2 reduced 14h at LHSV 317 h^{-1}

Time on stream (min)	45	90	135	180
Conversion (%)	59.66	57.36	55.31	53.66
Yield of product (%)				
Methane	6.22	5.79	5.46	5.50
Ethane	3.67	3.40	3.27	3.30
Ethylene	19.96	18.71	17.80	17.30
Propane	0.40	0.37	0.37	0.35
Propylene	14.18	13.40	12.87	12.04
Unknown	0.07	0.07	0.06	0.07
Butane	0.07	0.07	0.07	0.07
C_4 olefins	5.86	5.95	5.62	5.19
Butadiene	1.37	1.34	1.39	1.40
C_5 olefins	4.88	5.24	5.36	5.39
C_{6+}	1.47	1.51	1.54	1.55
Coke	1.51	1.51	1.51	1.51

(Reaction condition; Packing 0.5Pt/TiO_2 @550°C, Pressure: 1 atm, feed rate of H_2O: 13.1 mL/h, *n*-hexane: 18.0mL/h, LHSV: 268h^{-1})

APPENDIX D

CATALYST CHARACTERIZATION

D1. XRD diffraction pattern of TiO_2 catalyst

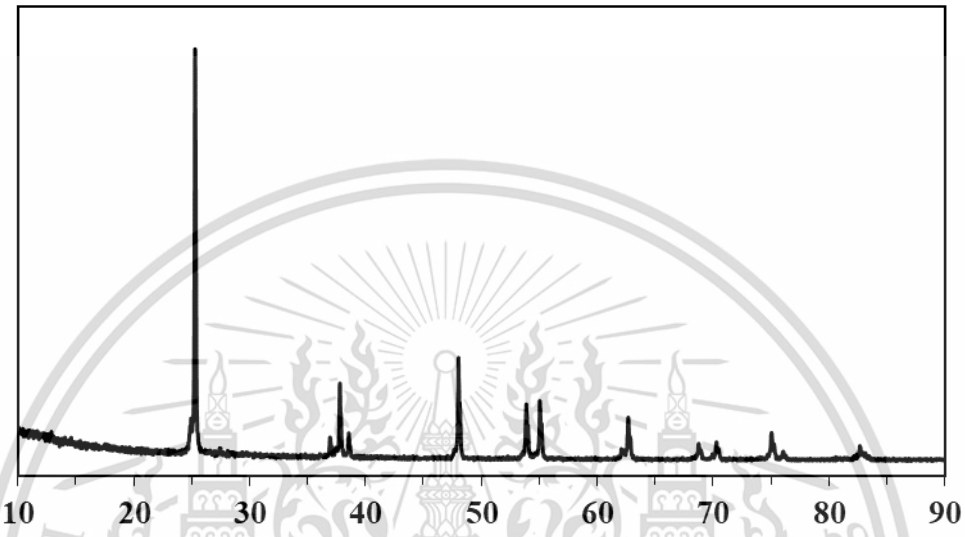

Figure D1 XRD patterns of TiO_2

D2. XRD diffraction pattern of ZrO_2 catalysts

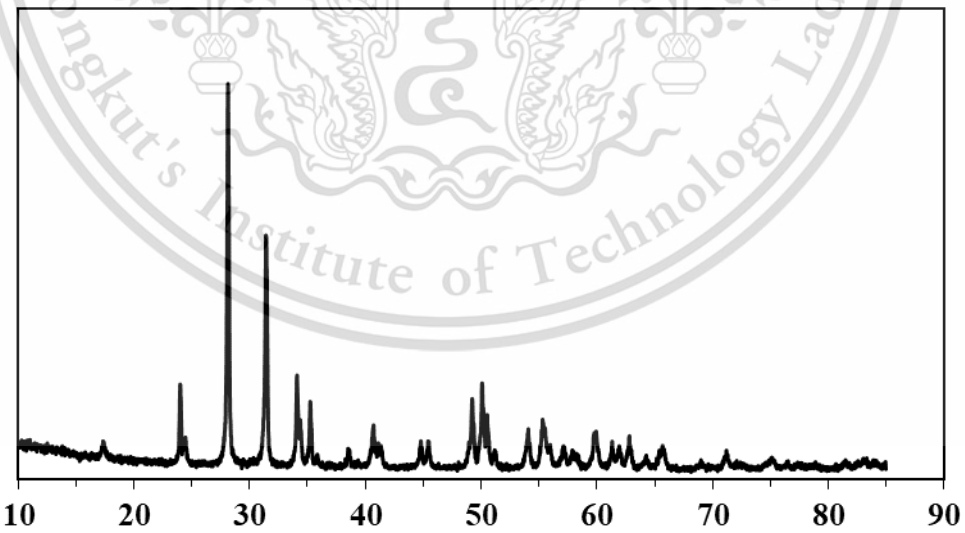

Figure D2 X-ray diffraction pattern of ZrO_2

D3. XRD diffraction pattern of SiO_2 catalysts

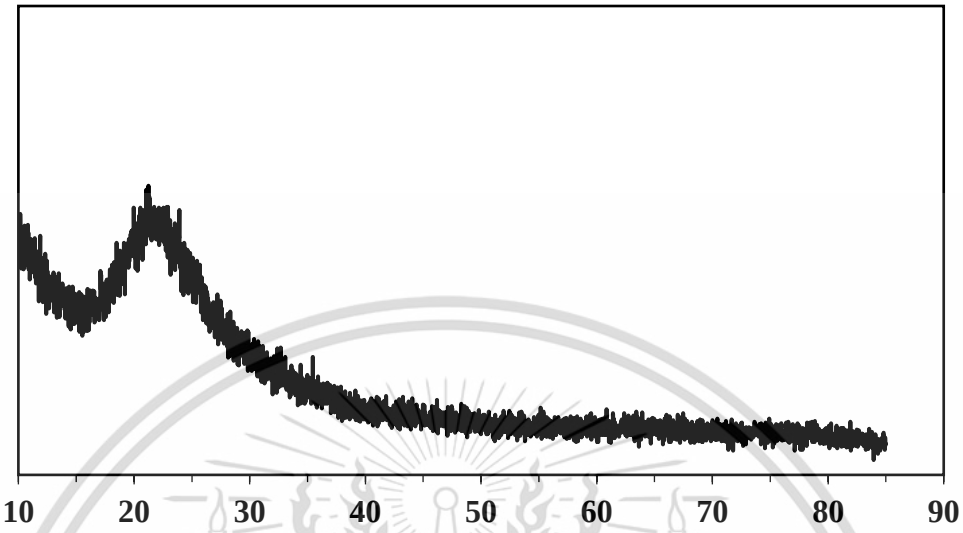

Figure D3 X-ray diffraction pattern of SiO_2

D4. XRD diffraction pattern of 0.5Pt/TiO_2 catalysts

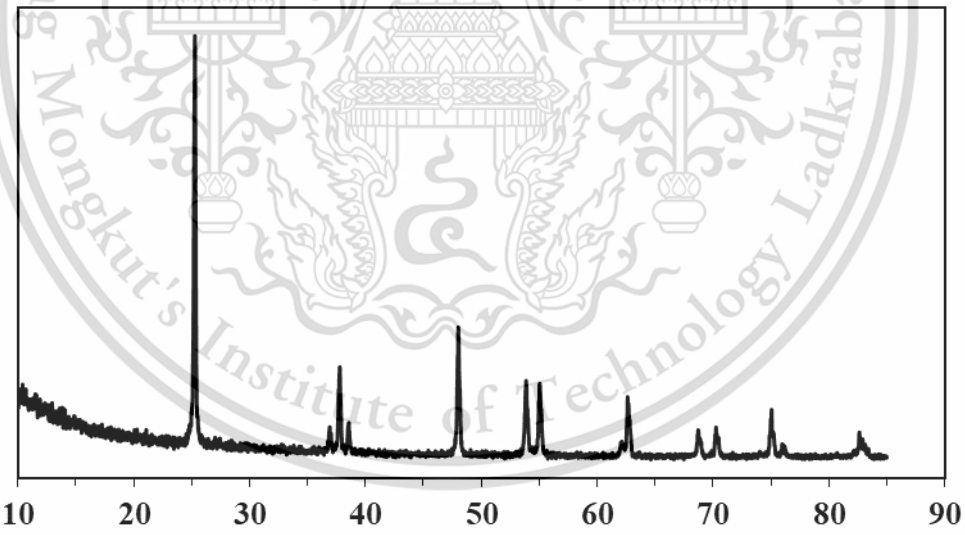

Figure D4 X-ray diffraction pattern of 0.5Pt/TiO_2

D5. Nitrogen adsorption-desorption (BET)

Table D1 Surface area analysis by nitrogen adsorption/desorption technique

Catalyst	Specific surface area (m^2/g)
SiO_2	300.0
TiO_2	17.6
ZrO_2	5.5
$0.5Pt/SiO_2$	280.1
$0.5Pt/TiO_2$	10.6
$0.5PtZrO_2$	4.9

D6. Inductively Coupled Plasma (ICP)

Table D2 Elemental analysis by Inductively Coupled Plasma technique

Catalyst	Pt Content (by %weight)
$0.5Pt/SiO_2$	0.4
$0.5Pt/TiO_2$	0.4
$0.5PtZrO_2$	0.5

D7. Transmission electron microscopy (TEM)

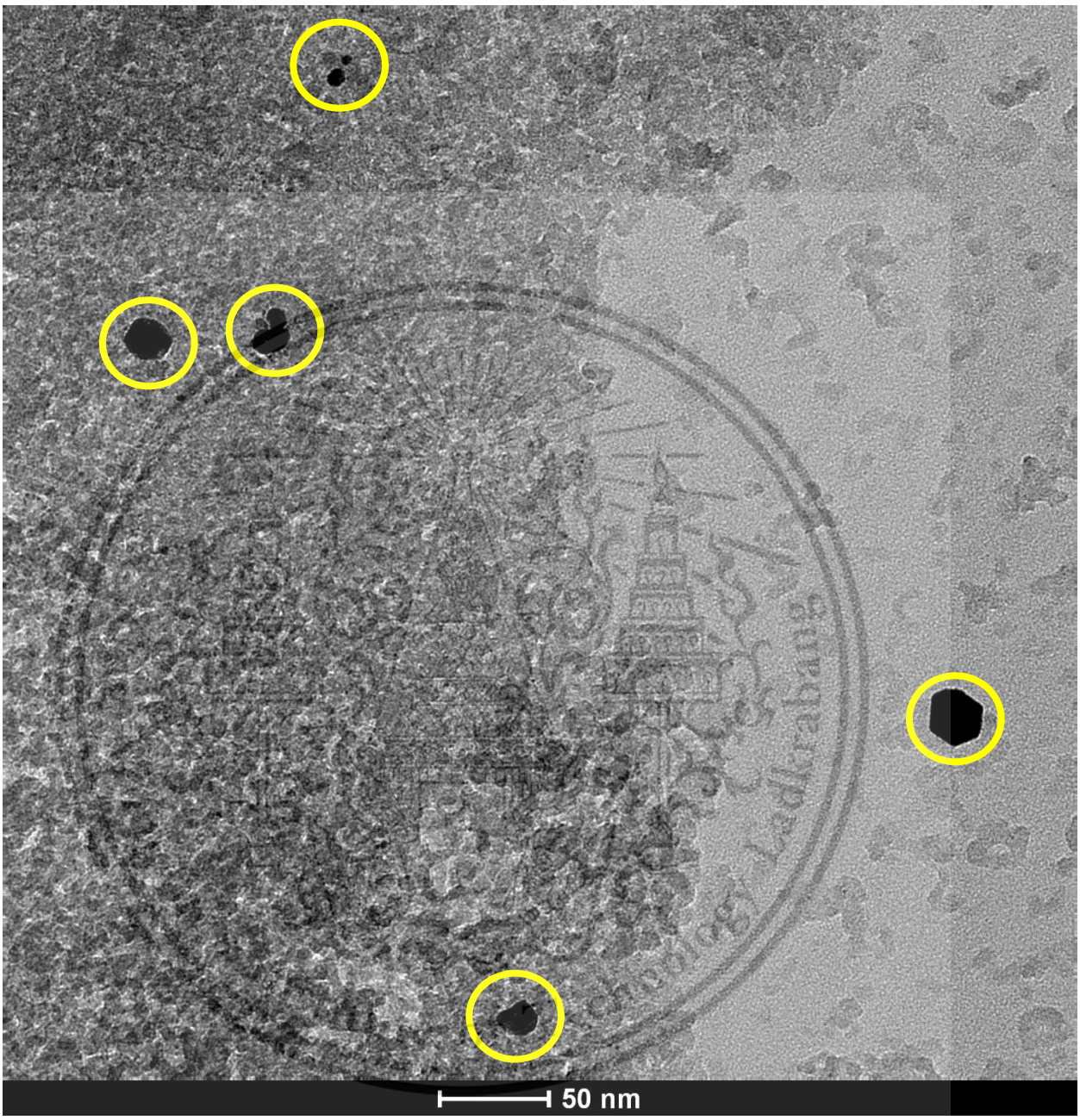

Figure D5 TEM image of 0.5Pt/SiO_2 (reduced for 5h)

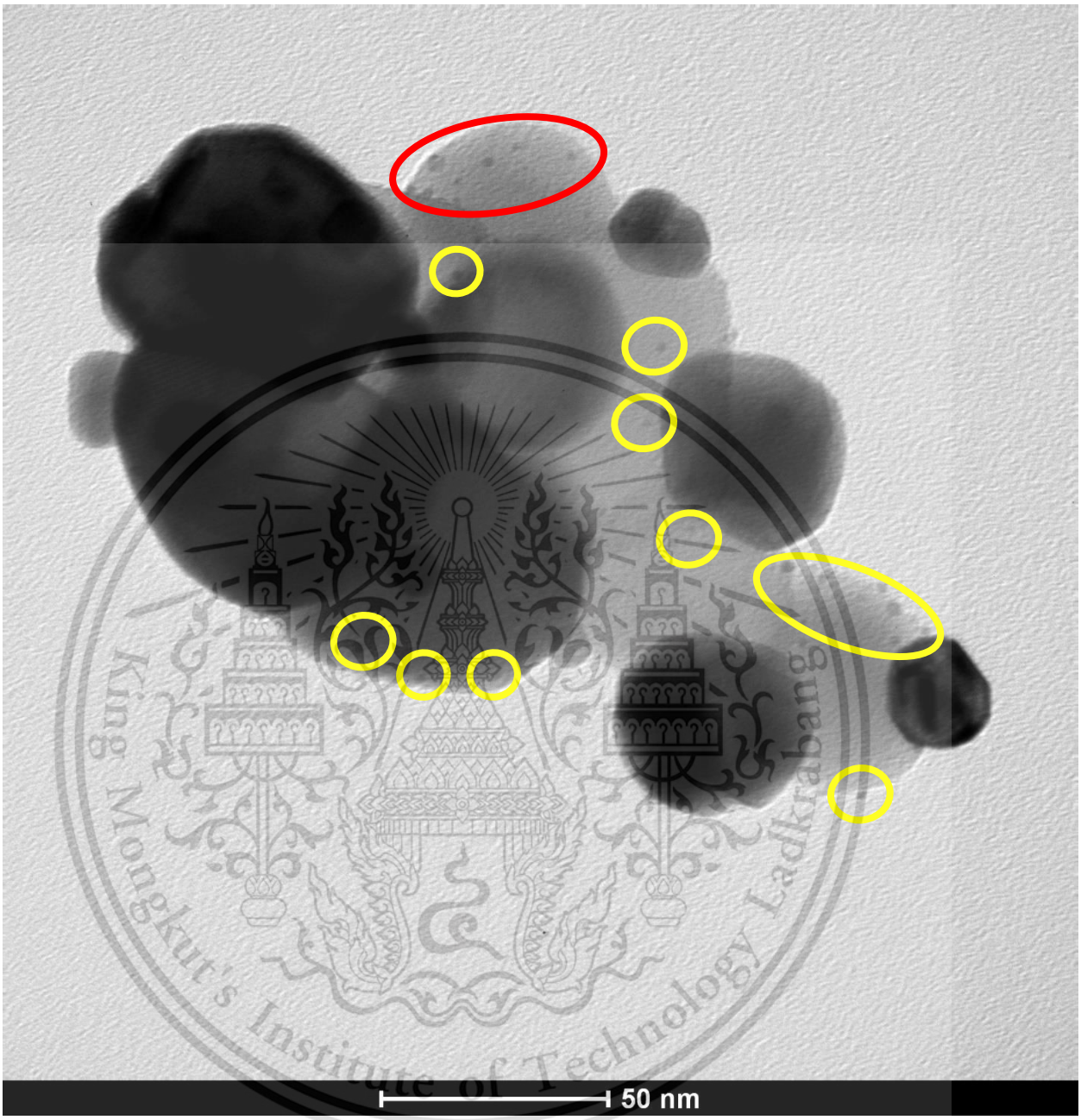

Figure D6 TEM image of 0.5Pt/ZrO_2 (reduced for 5h)

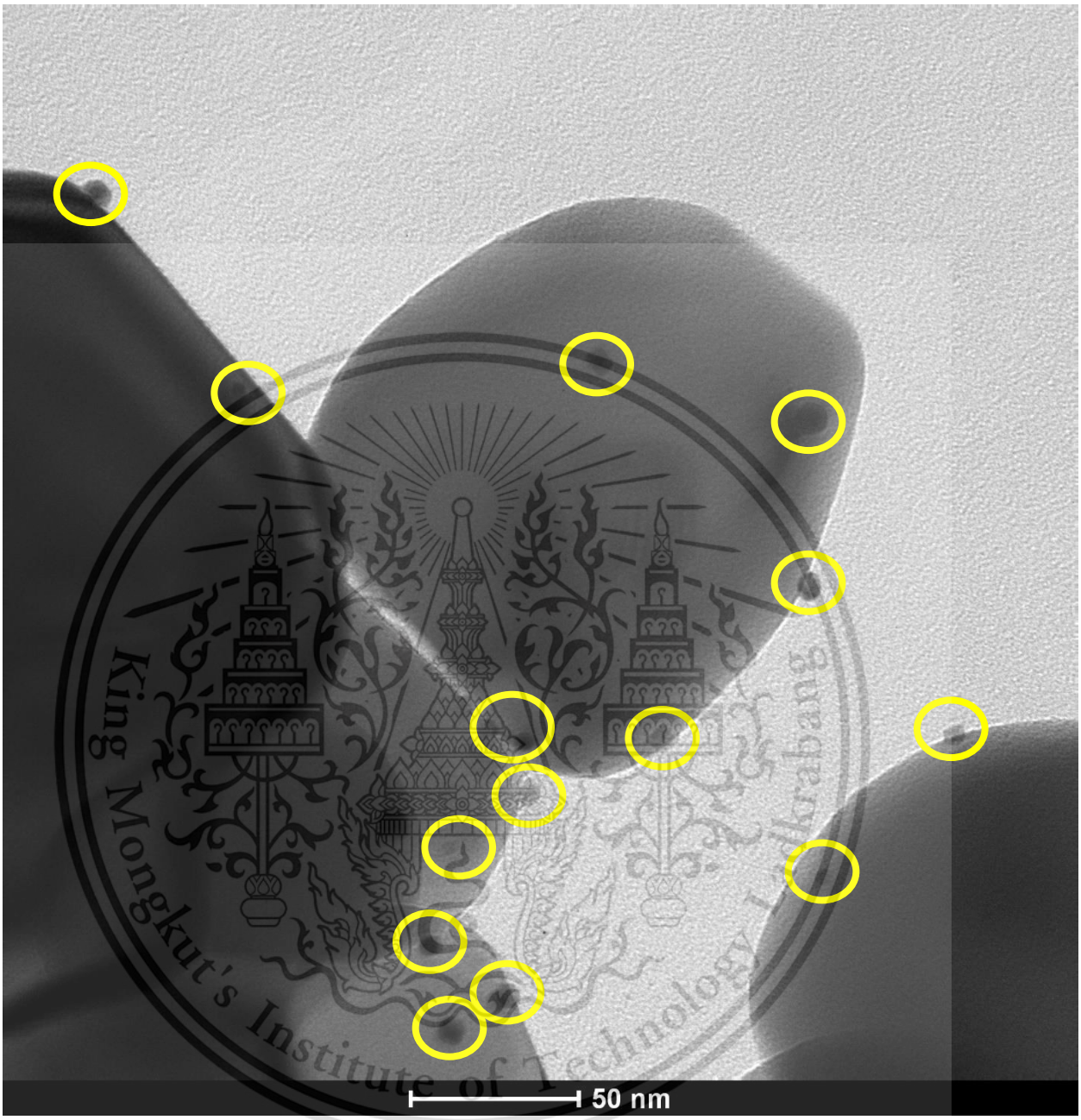

Figure D7 TEM image of 0.5Pt/TiO_2 (reduced for 1h)

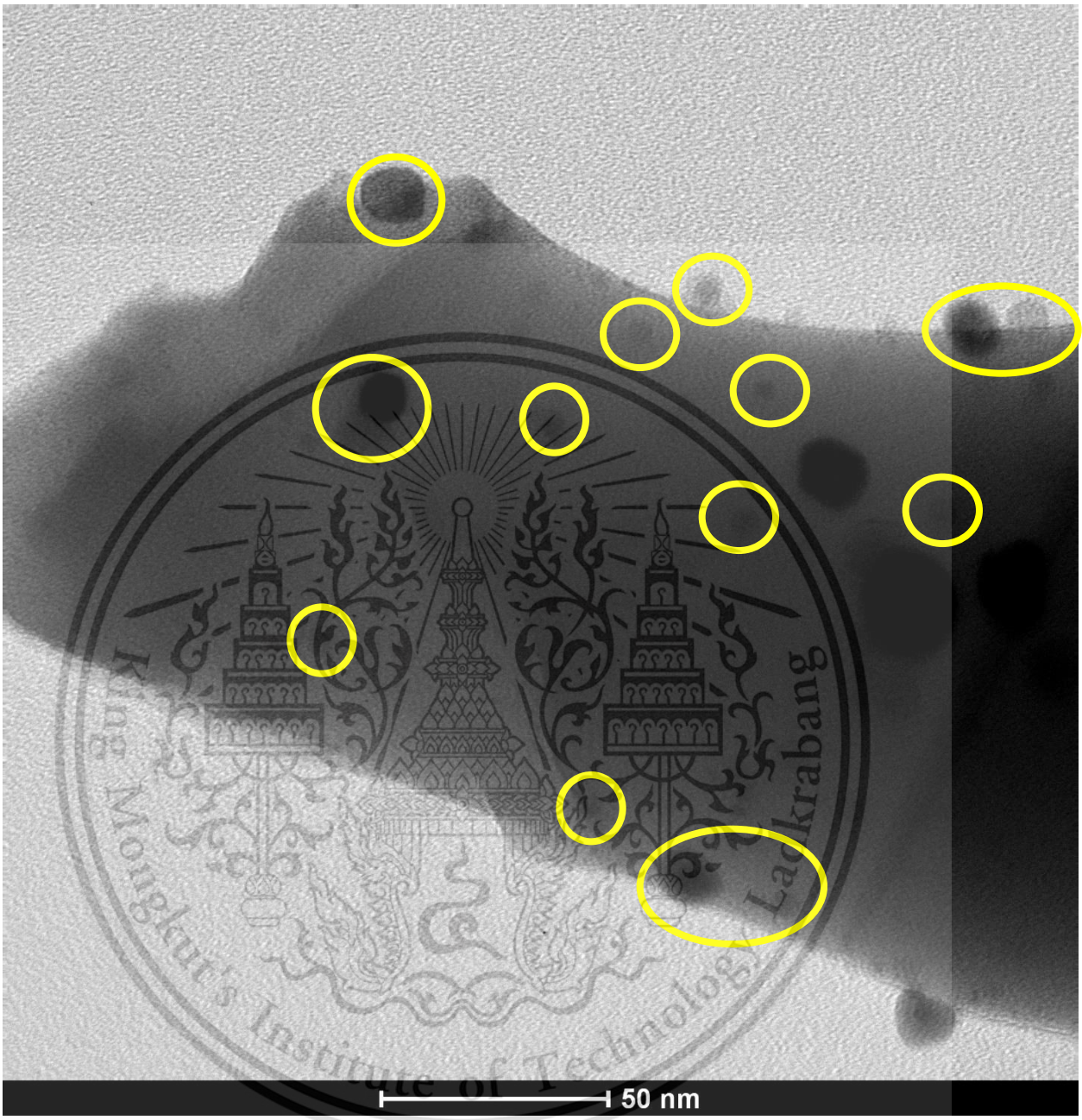

Figure D8 TEM image of 0.5Pt/TiO_2 (reduced for 5h)

Figure D9 TEM image of 0.5Pt/TiO_2 (reduced for 14h)

D8. Temperature program reduction (H_2-TPR)

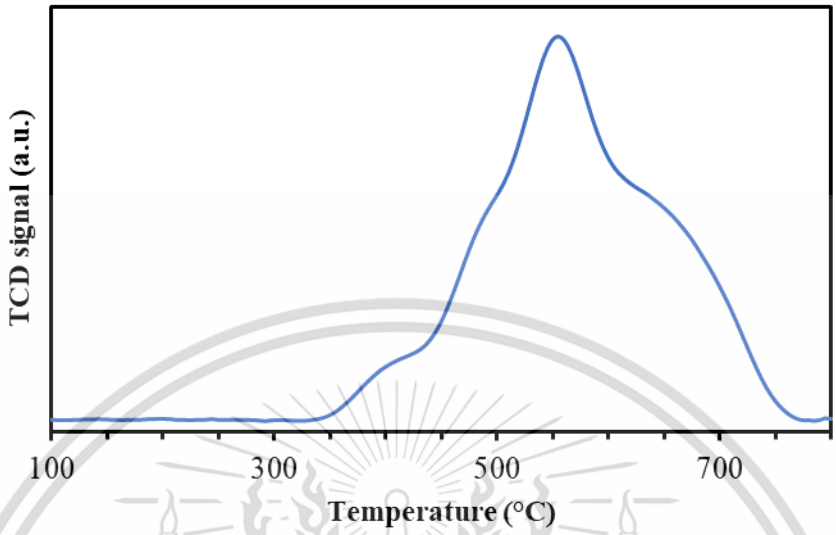

Figure D10 H_2-temperature programmed reduction profile of TiO_2

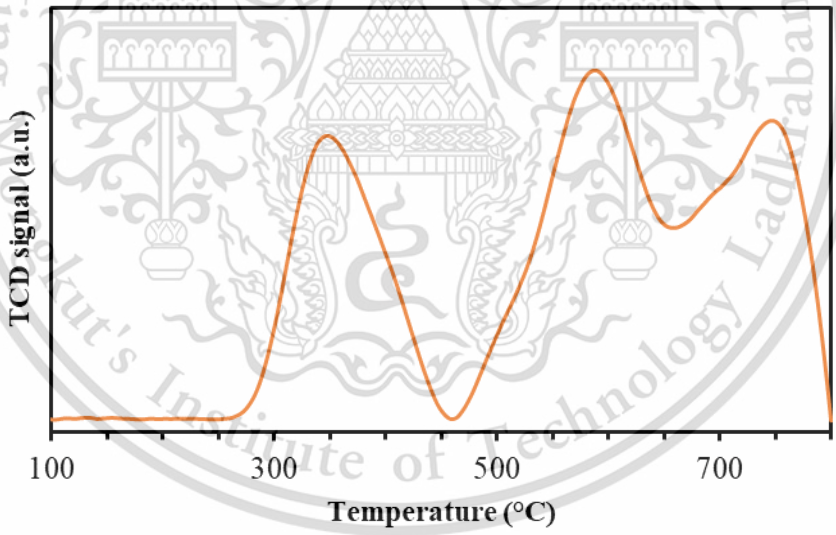

Figure D11 H_2-temperature programmed reduction profile of 0.5Pt/TiO_2

Author Biography

Name	Mr. Teerud Panjanapongchai
Date of Birth	24 January 1995
Address	61 Soi Charoennakorn 40, Banglumphulang Subdistrict, Klongsan District, Bangkok Province, 10600
Education	(2017) Bachelor of Science in 2.71 KING MONGKUT'S INSTITUTE OF TECHNOLOGY LADKRABANG (2021) Master of Science in 3.43 KING MONGKUT'S INSTITUTE OF TECHNOLOGY LADKRABANG

Academic Publication

1. T. Panjanapongchai, T. Sooknoi, T. Maluangnont. "Catalytic steam cracking of n-hexane over platinum catalysts" The 26th PPC Symposium on Petroleum, Petrochemicals, and Polymers and The 11th Research Symposium on Petrochemical and Materials Technology (PPC 2020), pp. 103-108